T H E U N I V E R S I T Y O F M I C H I G A N

COLLEGE OF ENGINEERING
Department of Engineering Mechanics
Department of Mechanical Engineering

Tire and Suspension Systems Research Group

Technical Report No. 1

PRELIMINARY MEASUREMENTS ON HEAT BALANCE IN PNEUMATIC TIRES

G. H. Nybakken
D. Collart
R. J. Staples
J. I. Lackey
S. K. Clark
R. N. Dodge

supported by:

NATIONAL AERONAUTICS AND SPACE ADMINISTRATION
LEWIS RESEARCH CENTER
GRANT NO. NGR 23-005-417
CLEVELAND, OHIO

administered through:

OFFICE OF RESEARCH ADMINISTRATION ANN ARBOR

September 1971

TABLE OF CONTENTS

LIST OF ILLUSTRATIONS

LIST OF ILLUSTRATIONS (Continued)

LIST OF ILLUSTRATIONS (Concluded)

I. INTRODUCTION

The purpose of the analysis and measurements outlined in this report is to give a clearer picture of the origin of heat generation in a pneumatic tire, and of the way in which the heat leaves the tire. In more detailed form, this question breaks down into several individual questions or research studies, each worthy of substantial effort. These may be expressed as:

(1) To what extent is heat generated by hysteresis within the tire tread and side walls, and to what extent by mechanical scuffing between outer tread surface and roadway?

(2) What is the distribution of release of heat by hysteresis relative to depth beneath the outer tread surface?

(3) To what extent does the total heat generated flow to the atmosphere, and to what extent does it flow through the contact patch into the roadway?

Subsequent sections of this report attempt to throw light on these questions by both analytical and experimental means.

II. SUMMARY OF RESULTS

Research on this problem has been directed along three major lines of activity. These are:

(1) An analytical study of the problem of heat conduction in the rolling tire as it contacts the roadway.

(2) Experimental measurements on full sized tires.

(3) Experimental measurements on small scale, model tires.

In regard to these three phases of effort, the analytical studies so far have been the least productive, at least in terms of generating new information. They have, however, been extremely helpful in interpreting the results of some of the experiments carried out under this program. For example, a number of analytical solutions to thermal conductivity problems have been developed during the course of this one year of effort. In particular, the problem of two-body contact has been studied in some detail and a computer program written to give the temperature distribution in two bodies in contact for a short period of time, under conditions of heat release at the surface of these two bodies and under conditions of an elevated temperature of one body with respect to the other. In general this work shows that for the velocities and thermal conductivities encountered by an aircraft tire operating on a runway, the temperature profile caused by surface heating is that of an extremely thin skin on both surfaces, with the proportion of heat flowing into the concrete runway and into the tire being governed by their relative thermal conductivities and specific heats. This gives rise to the expectation that such

a thermal proportioning could be radically affected by controlling the thermal properties of the runway itself, even in the form of a very thin skin or sheet. So far, however, it has not been possible to calculate in any reasonably sound way the degree of heat released from the tire due to surface scrubbing on the runway, and so one must rely upon measured values of this quantity in order to examine the various temperature profiles exhibited.

Experiments on fully instrumented passenger car tires were carried out at the Texas Transportation Institute using The University of Michigan Highway Safety Research Institute Mobile Tire Tester. Instrumentation in these tires consisted of a large number of thermocouples embedded throughout the thickness of the tread and carcass at two regions, as well as an array of thermocouples around the meridional section of the tire. These tires were run for fairly long periods of time at a speed of 50 mph, and both the initial transient temperature rise profile as well as the near-equilibrium temperature distribution were measured.

From the results of the transient temperature work it has been possible to show that a very large fraction of the total work done in rolling the tire under straight line, unbraked conditions is made up of hysteretic heat distributed throughout the tire carcass. However, far and away the largest fraction of this heat appears to be located close to the tread surface of the tire, opening up the possibility that it could be removed by some highly conductive surface mechanism.

The exact fraction of heat so generated cannot be defined quantitatively until further experiments accurately define the total drag force of the tire

at the velocity and load conditions used in the thermocouple measurements.

These conclusions based on thermocouple measurements are substantiated by thin film temperature sensor measurements taken directly on the highway. A series of these measurements show that the temperature rise associated with a freely rolling tire of typical passenger car size, at a speed of 50 mph and loaded with a vertical load of 1000 lb, was so small as to be barely measurable. The sensitivity of these sensors is less than 1°F, so that we can state with certainty that the temperature rise is less than this 1°F limit. Calculations are not yet complete on this data, but it strongly implies that surface scrubbing itself plays a very small part in the rolling loss process.

Slow speed scratch measurements were made using the same tire as used in the thermocouple measurements. These were carried out on the flat plank tire testing machine at The University of Michigan Highway Safety Research Institute, also under the same vertical load as was used on the highway tests. These measurements showed that the drag force associated with surface scrubbing of the tire was less than 10% of the total drag force of the tire. This implies that less than 10% of the energy used to move the tire forward is released in the form of surface heat scrubbing. This confirms the two previous experimental conclusions, but still leaves the possibility open that the hysteretic portion of the tire loss, which appears to be the largest portion by far, has its origin very close to the surface.

Recent computational studies on the stress states near the surface of rolling tires, such as that of Yandell [1], reinforces the idea that the distribution of hysteretic and frictional losses may be radically different in a

pure rolling and a pure sliding tire. Therefore, the conclusions reached so far in this work must be considered only for the case of the rolling tire and not as general statements good for all operating conditions.

III. THERMOCOUPLE MEASUREMENTS

A series of experiments was conducted to examine the internal heating of a tire carcass under various conditions. The tires were instrumented with thermocouples bonded into the carcass. The temperature was recorded as a function of time and from this data the rate of heat generation could be calculated. This rate of heat generation can be compared to the mechanical power dissipated.

The experiments were conducted on regular roads using The University of Michigan Highway Safety Research Institute Mobile Tire Tester, a truck modified to carry a tire under various loads and alignments at normal highway speeds.

A total of three tires was instrumented and yielded useful information in the tests. Two of the tires, identical B. F. Goodrich G78-15 bias belted tubeless tires mounted on 6JK pressed steel rims, were instrumented in the same way. They bore code numbers DG24-0026-5 G598 and DG24-0026-8 G598 and are identified by the abbreviations G78-15 #5 and G78-15 #8, respectively. These two tires had a solid tread surface with the same gross contour as the standard production tire, but without grooves or sipes. The third tire was an H78-15 of the same construction as the G78-15 tires and was mounted on the same rim. This tire had a standard production tread. All three tires were load range B tires and the two sizes are both common on domestic intermediate size automobiles.

The thermocouple locations relative to the cross-section for the G78-15 tires and the H78-15 tire are shown in Figures 1 and 2, respectively.

A fourth tire, a B. F. Goodrich 7.75-14 bias belted tubeless tire (code number R86-4079-3 U304) was instrumented but was not used because a leak developed during preliminary testing.

The tires carried 1000-lb vertical load and were inflated to 24 psi except as otherwise noted.

The thermocouples were installed in the following way: the immediate area of the chosen location was frozen with liquid nitrogen, a 1/8 in. hole was drilled to the proper depth, the tire was allowed to return to room temperature and, after the thermocouple was inserted, the hole was potted with Duro Plastic Rubber (T.M.). The Plastic Rubber was injected with a syringe to avoid trapping air pockets.

All holes were drilled from the inside of the tire. In those locations where the thermocouple was within or beyond the ply structure, the fabric was also drilled.

Those thermocouples located on the interior wall of the carcass were glued using Plastic Rubber into shallow dimples machined into the surface.

The thermocouples were made from 28-gauge copper-constantan twin lead wire with plastic insulation. The junctions were butt-welded electrically and that region stripped of insulation during the welding process was coated with "Gaugecoat," a thin latex rubber waterproofing agent.

The wire leads were taken from the point where they emerged from the rubber, around the inside of the tire to the common exit holes in the rim.

There were two such exit holes for the G78-15 tires and one for the more lightly instrumented H78-15 tire. The wires passed through the holes in a bundle and the hole region was potted with Plastic Rubber which served as a grommet, seal, and mechanical reinforcement.

The lead wires were fastened to the inside of the tire at 6-in. intervals using tape secured with Eastman 910 adhesive. Preliminary experiments showed that a small amount of slack between these fastening points was necessary to permit the lead wires to flex with the tire and to prevent breakage.

The constantan lead wires were fastened to a common junction inside the tire cavity and a single constantan lead wire was brought out from this junction.

After passing through the exit holes the wire bundle was brought to a slip ring assembly, thence to a 32°F ice bath reference junction located on the rear of the truck, and finally to the instrumentation in the cab of the truck.

The instrumentation in the truck consisted of a low resistance multipole switch, a digital microvolt meter, a stop watch, and a tape recorder. The switch position and corresponding voltage and time were read verbally into the recorder for later transcription.

The experiments reported here were performed on three occasions. The experiments using the H78-15 tire were performed on November 19, 1970, and December 3, 1970, at Ann Arbor, Michigan, on concrete roads with air temperatures between 40° and 45°F. The experiments using the G78-15 tires were performed March 1, 1971, through March 3, 1971, inclusive, at College Station,

Texas, on asphalt roads with air and road temperatures in the ranges 40°-70°F and 45°-90°F, respectively.

The experiments were conducted by bringing the truck to the appropriate speed, at which point the tire was lowered to the pavement and run under load at a constant speed until the appropriate data had been taken. The tire was then lifted and allowed to reach a uniform temperature as determined by the thermocouples before a second experiment was conducted.

The recorded thermocouple potentials were transcribed and converted to degrees Fahrenheit and plotted as temperature vs. time. The data for the initial 1 to 2 min were examined to determine if conduction, diffusion, and convection effects were sufficiently small to warrant further processing of the data. If the graphs were sufficiently straight and did not exhibit curvature or the exponential leveling off associated with heat flow, then it was assumed that the rate of temperature increase was representative of the initial input of heat.

It should be noted that, barring heat flow, the conversion of a constant mechanical power input to thermal energy yields a constant rate of temperature increase independent of initial temperature of the tire, and the ambient road and air temperatures.

The rate of temperature increase was determined by fitting a straight line to the temperature vs. time graph and determining the slope of this line or by taking the temperature difference between two data points spaced 60 or 80 sec apart and directly calculating $\Delta T/\Delta t$. The two methods are almost equivalent and the choice of method was made subjectively according to the

almost the same value and because the first scheme was much easier to use and because the difference between the values obtained using the two schemes was less than the overall projected uncertainty in the whole experiment, it was decided to use the first scheme for all the calculations of heat influx.

The second scheme is illustrated in the Appendix. The partitioned sections used are shown in Figure 1 which also shows thermocouple locations.

Experiments were conducted with the tires rolling free, with the tires at yaw angles of 4° and 8°, and with brake torques yielding drag forces up to 460 lb. The speeds used were 30 and 50 mph. Drag force could be measured for either nonzero yaw or nonzero brake torque but was too small to be measured for the free rolling case. The drag of the free rolling tire was assumed to be 20 lb, equal to 2% of the 1000-lb vertical load.

Samples of the data and the graphs derived from them are shown in the figures and tables.

Figure 3 gives an example of the temperature vs. time data for thermocouples located around the cross section and Figure 4 gives an example of temperature vs. time data for points within the crown. Both these figures refer to a free rolling tire.

Figures 5 and 6 show sample temperature and heat generation profiles, respectively, through the crown of the tire. The specific rate of heat generation is the product of the rate of temperature increase and the specific heat capacity.

The total heat generation data for the free rolling tire is presented in Table I along with the power input based on 20 lb drag and 50 mph forward

speed. The heat generation is calculated according to Eq. (1). Despite the extent of the assumptions involved there is surprisingly close agreement between the heat generated and the mechanical energy expended. The mean deviation for the $\Delta T/\Delta t$ data is 9% and it follows that the same mean deviation is applicable for the Q values. If the drag was indeed constant for all the experiments the average Q/P value has a mean deviation of 9%. This fact coupled with the average Q/P value of 1.035 indicates that the majority of mechanical energy used to drive a free rolling tire is converted to heat via tire rubber and fabric hysteresis.

The data in Table II represents the heat generation around the cross section for various yaw and braking conditions for the G78-15 #5 tire. The drag was measured using the equipment on the Mobile Tire Tester. The power expenditure is meaningful only for the yawed experiments because in the braked experiments the brake mechanism absorbs an unknown fraction of the total mechanical energy.

However, the yawed experiments may be compared with the unyawed experiments. Here we see that only 36% of the mechanical energy is converted into carcass heat whereas the figure for an unyawed tire was close to 100%. The difference is apparently due to the increased scrubbing in the contact patch in the yawed case.

Table III contains a summary of some pertinent experiments with the H78-15 tire which was instrumented in the shoulder region. The experiments were all conducted at 30 mph with the standard 1000-lb vertical load and 24 psi inflation pressure. The heat generation rate Q was determined by using

Eq. (1). The thermocouple locations are referenced in Figure 2. The power figure for the free rolling tire corresponds to 20 lb drag.

Note that the drag force may be under-estimated because the Q/P ratio indicates a surplus of 13%. However, the Q/P data for both the free rolling and yawed rolling tests compare well with the data for the corresponding tests with the G78-15 tires considering the extent of the uncertainties involved in the tests.

Most of the experiments were of less than 5 min total duration because diffusion and convection effects would only complicate the determination of heating effects as explained previously. However, one experiment was conducted for a time sufficient to reach thermal equilibrium.

Temperature profiles through the crown showing the approach to equilibrium are shown in Figure 5. Note that as diffusion within the tire and heat transfer out of the tire become important, the hottest point in the crown moves from the region close to the surface inward toward the middle of the cross section. The profile yields temperature gradient data which indicates that at equilibrium about 78% of the radial heat flow is toward the outer surface and the remaining 22% is toward the inner surface.

TABLE I

SUMMARY OF EXPERIMENTS WITH FREE ROLLING TIRES

0° yaw, no braking; 50 mph
Test #8 with G78-15 #8; all other tests with G78-15 #5

Test	Location									Avg. of 1-9	Q, ft lb/sec	P, ft lb/sec	Q/P
	1	2	3	4	5	6	7	8	9				
6	.0875	.1875	.2000	.1250	.1188	.1250	.2063	.1250	.1570	.1570	1760	1468	1.200
7	.0625	.1438	.1313	.1188	.0688	.0938	.1688	.2250	.1000	.1263	1416	1468	.965
11A	.1175	*	.2050	.1250	.0900	.1250	.2050	*	.1900	.1511	1692	1468	1.152
13	.0775	*	.1613	.1188	.1025	.1238	.1950	*	.1088	.1268	1420	1468	.968
1	.0688	.1375	.1250	.1000	.1063	.1125	.1688	.2063	.1125	.1264	1417	1468	.965
8	.0625	.1750	.1063	.1188	.1313	.1375	.1500	.1438	.1375	.1290	1446	1468	.986
Avg.						Average of six experiments →				.1357	1520	1468	103.5

Q is calculated according to Eq. (1). It is the rate of increase of the total heat energy within the tire structure.
P is the product of the total drag and velocity.
*Thermocouple inoperative. This location omitted from average.

TABLE II

SUMMARY OF EXPERIMENTS WITH YAWED OR BRAKED TIRES

Tire G78-15 #5, 50 mph
Values of $\Delta t/\Delta t$, °F/sec

Test	Yaw, deg	Brake*	Drag No.	Location								Q, ft lb/sec	P, ft lb/sec	Q/P
				1	3	4	5	6	7	9	Avg. of 1-9			
10	4	0	70	.1750	.2875	.1613	.1175	.1600	.1650	.0900	.1652	1850	5140	.360
12A	8	0	112	.2375	.3613	.2575	.2238	.2963	.2838	.1988	.2656	2970	8210	.362
11A	0	✓	70	.0775	.1475	.1050	.0863	.1050	.1913	.1000	.1161	.290	5140**	.252**
12B	0	✓	112	.0775	.1100	.0650	.0500	.0663	.1125	.0688	.0786	870	8210**	.106**

Q is calculated according to Eq. (1). It is the rate of increase of the total heat energy within the tire structure.

P is the product of the total drag and velocity.

*A check (✓) indicates that the brake was applied.

**No attempt has been made to determine the power dissipated in the braking system. Hence, this P does not represent power absorbed by the tire.

TABLE III

SUMMARY OF EXPERIMENTS WITH H78-15 TIRE AT 30 MPH

$\Delta T/\Delta t$, °F/sec

Test	Yaw, deg	Brake*	Drag No.	Location									Avg. of 1-9	Q, ft lb/sec	P, ft lb/sec	Q/P
				1	2	3	4	5	6	7	8	9				
18	0	0	D_o[b]	.0875	.1125	**	.1250	.0750	.0625	.0792	.0792	.0708	.0865	969	880	1.111
22[a]	0	0	D_o[b]	.1083	.1125	.1250	.1167	.0833	.0708	.0750	.0667	.0625	.0912	1042	880	1.182
15	0	✓	100	.0778	.1278	**	.1444	.0944	.0778	.0889	.0889	.0778	.0972	1090	4400	.248
24[a]	0	✓	100	.0611	.0833	**	.0944	.0611	.0389	.0500	.0500	.0444	.0604	628	4400	.154
17	4	0	90	.0944	.1000	**	.1667	.0722	.1556	.1722	.1444	.1444	.1312	1470	3960	.371
16	4	0	165	.1056	.1000	**	.2111	.0944	.2333	.2278	.2056	.2056	.1729	1935	7250	.267
23[a]	8	0	90	.0889	.0833	**	.1556	.0667	.1667	.1566	.1167	.1222	.1195	1340	3960	.338
Avg. of 18, 22	0	0											.0889	995	880	1.130

Q is calculated according to Eq. (1). It is the rate of increase of the total heat energy within the tire structure.
P is the product of the total drag and velocity.
*A check (✓) indicates that the brake was applied.
**Thermocouple inoperative. This location omitted from average.
[a]These tests were conducted with an improperly sealed system. Pressure dropped from 29 psi to approximately 24 psi for these tests.
[b]D_o is taken to be 20 lb equal to 2% of 1000-lb vertical load.

TABLE IV

SUMMARY OF EXPERIMENTS

Data Page No.	Date	Tire*	Yaw, deg	Brake**	Drag,+ lb	Side Force,++ lb	Velocity, mph	T_{road}, °F	T_{air}, °F	Load, lb	Pressure, psi
1	3/ 1/71	8	0	-	D_o	0	50	90	70	1000	22
2	3/ 1/71	8	4	-	64	647.5	50	95	70	1000	22
3	3/ 1/71	8	-	-	?	?	50	95	70	1000	24
4	3/ 2/71	14	0	-	D_o	0	50	51	43	1000	24
5	3/ 2/71	14	0	-	D_o	0	50	51	43	1000	24
6	3/ 2/71	5	0	-	D_o	0	50	46	40	1000	24
7	3/ 2/71	5	0	-	D_o	0	50	46	40	1000	24
8	3/ 2/71	5	0	-	D_o	0	50	46	40	1000	24
9	3/ 3/71	5	0	-	D_o	0	50	54	34	1000	24
10	3/ 3/71	5	4	-	70	?	50	65	41	1000	24
11A	3/ 3/71	5	0	-	D_o	0	50	65	41	1000	24
11B	3/ 3/71	5	0	✓	70	0	50	70	46	1000	24
12A	3/ 3/71	5	8	-	112	0	50	70	46	1000	24
12B	3/ 3/71	5	0	✓	112	0	50	70	46	1000	24
13	3/ 3/71	5	0	-	D_o	0	50	54	34	1000	24
14	3/ 3/71	5	0	-	D_o	0	50	54	34	1000	24
15	12/ 3/70	H	0	✓	100	0	30	54	34	1000	24
16	12/ 3/70	H	8	-	165	814	30	54	34	1000	24
17	12/ 3/70	H	4	-	90	555	30	54	34	1000	24
18	12/ 3/70	H	0	-	D_o	0	30	54	47	1000	24
19	This data page blank					0				1000	24
20	12/ 3/70	H	0	✓	460	0	40,50	54	47	1000	24
21	12/ 3/70	H	10	-	377	560	50	54	47	1000	24
22	11/19/70	H	0	-	D_o	0	30	54	~40	1000	28-18
23	11/19/70	H	4	-	90	555	30	54	~40	1000	29-22
24	11/19/70	H	0	✓	100	0	30	54	~40	1000	29-?
25	11/19/70	H	8	-	165	814	30	54	~40	1000	24

*G78-15 #5 → 5
G78-15 #8 → 8
H78-15 → H
7.75-14 → 14

**A check (✓) indicates that the brake was applied.

+D_o = Drag under free rolling conditions. This is assumed to be 20 lb and could not be measured accurately.

++Side force is assumed to be zero in all unyawed cases.

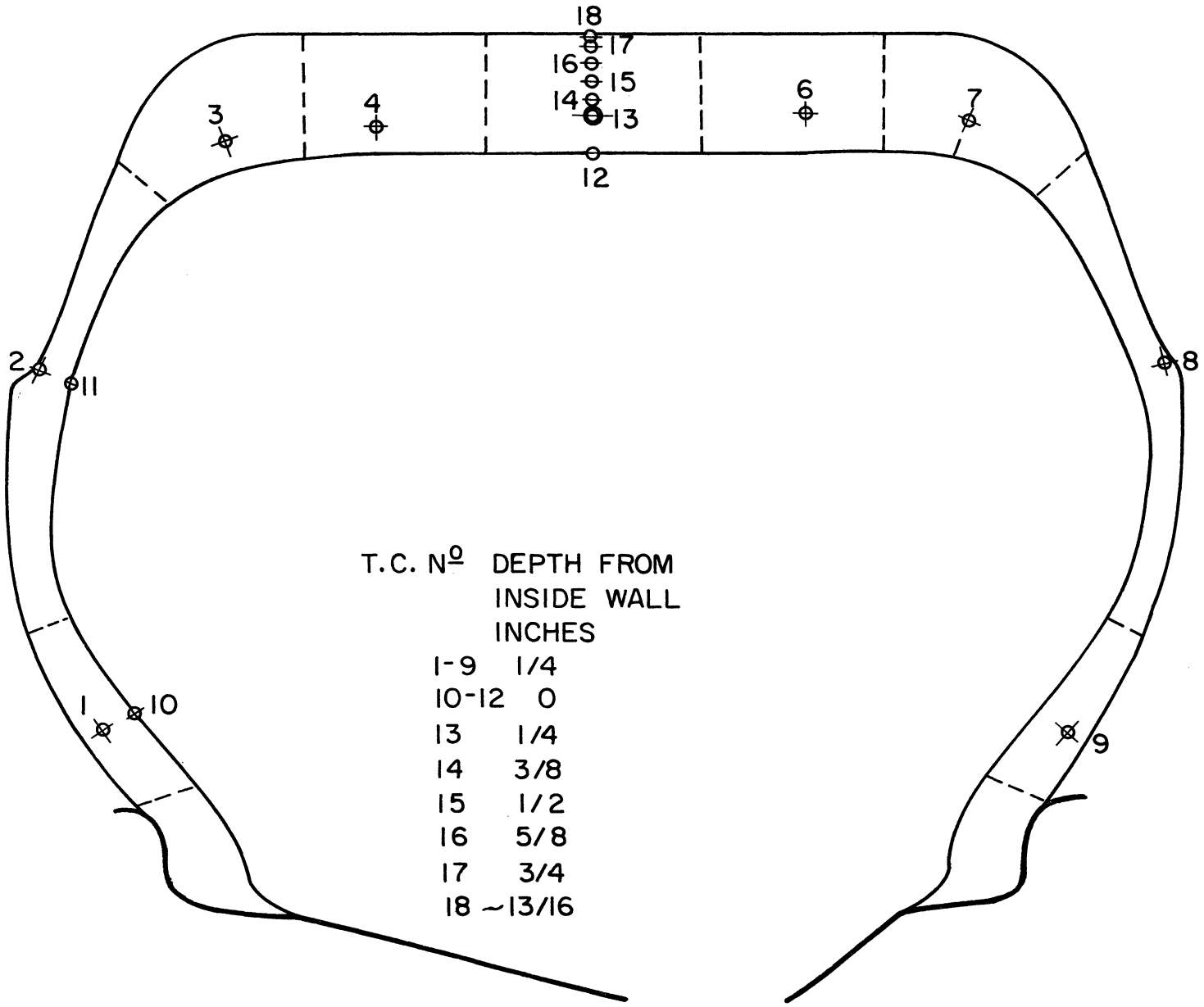

Figure 1. Thermocouple locations relative to cross section for G78-15 #5 and #8 on 6JK rim.

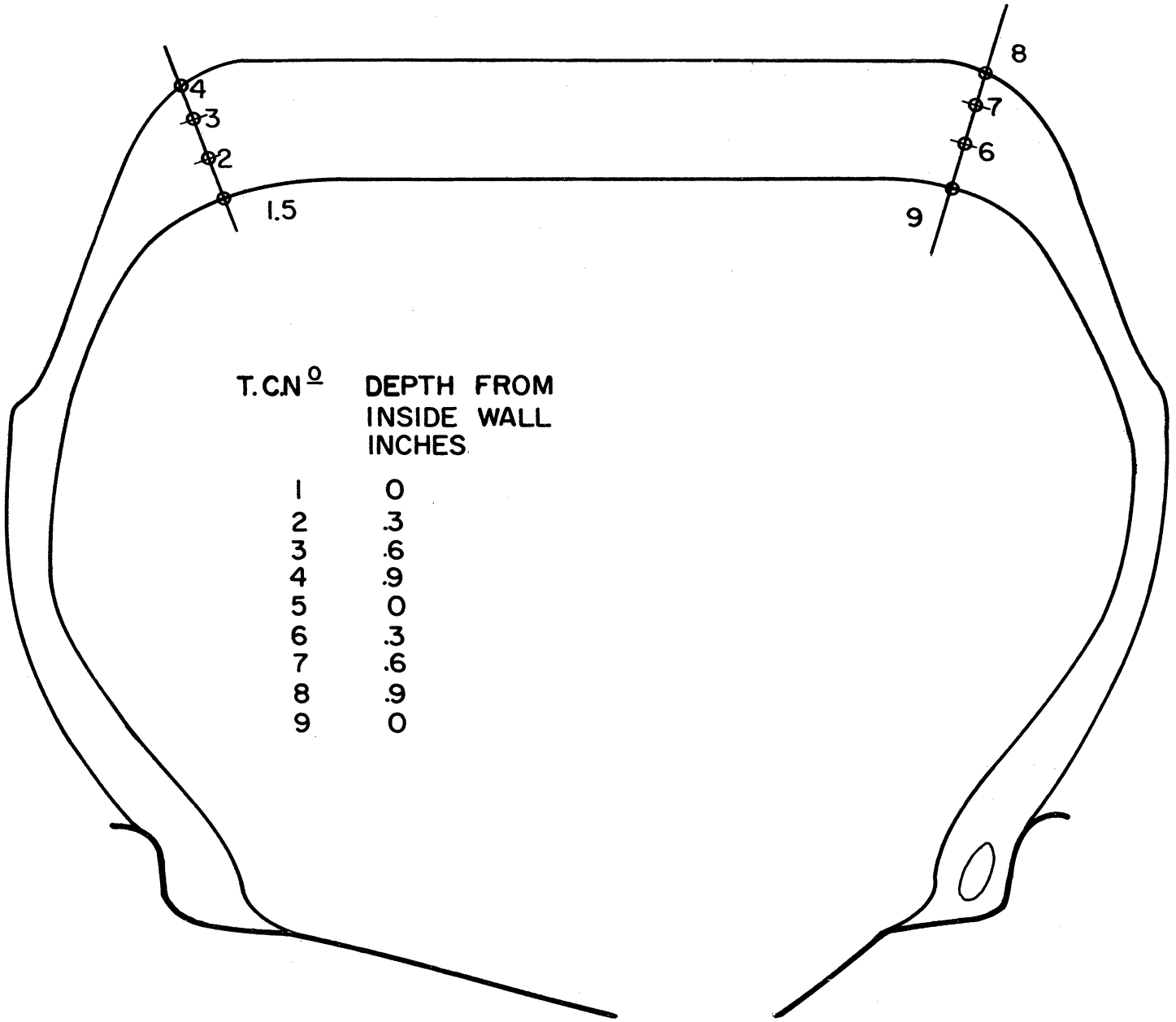

Figure 2. Thermocouple locations relative to cross section for H78-15 on 6JK rim (shown on a tracing of a G78-15 on a 6JK rim).

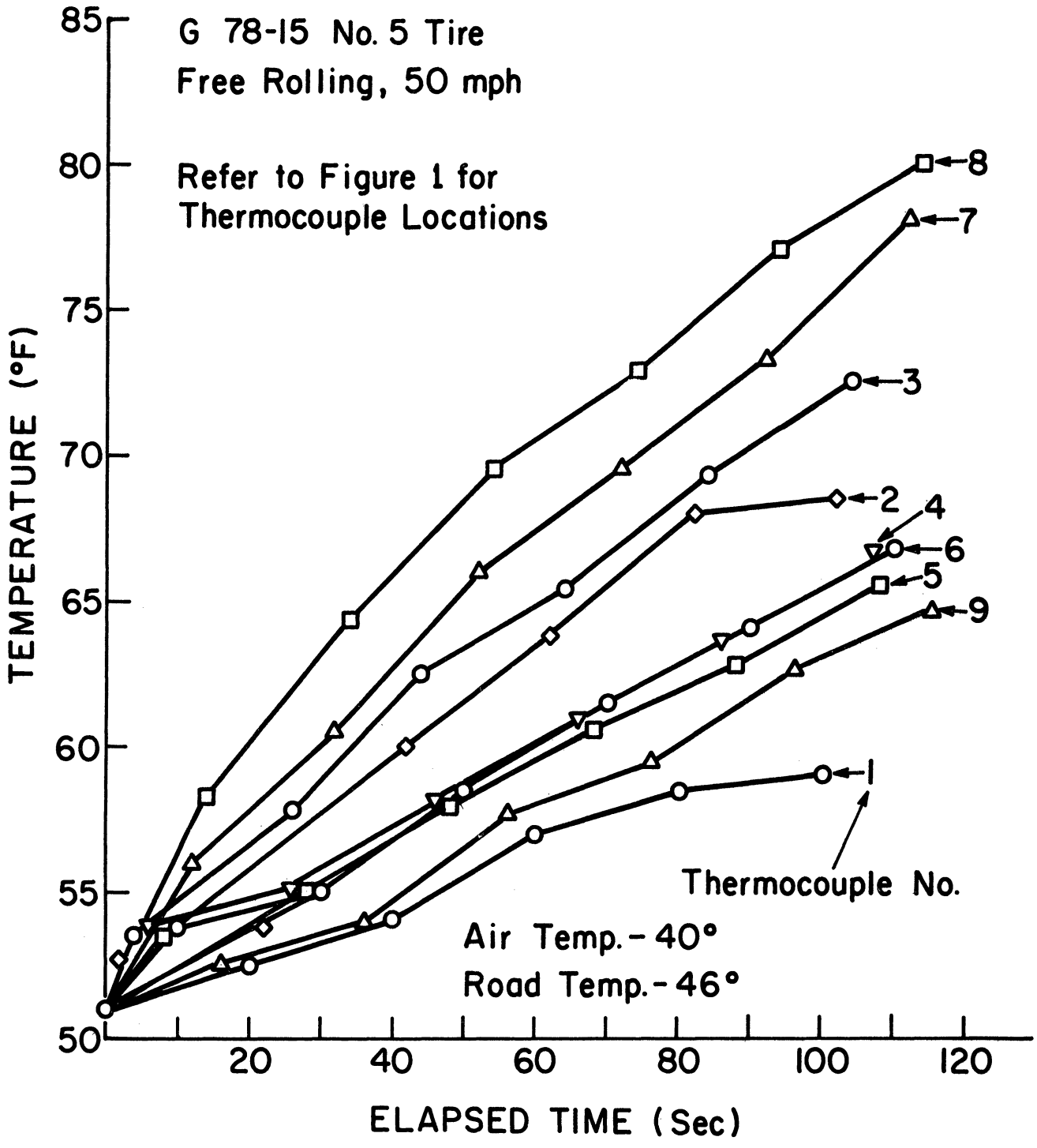

Figure 3. Temperature build-up around cross section.

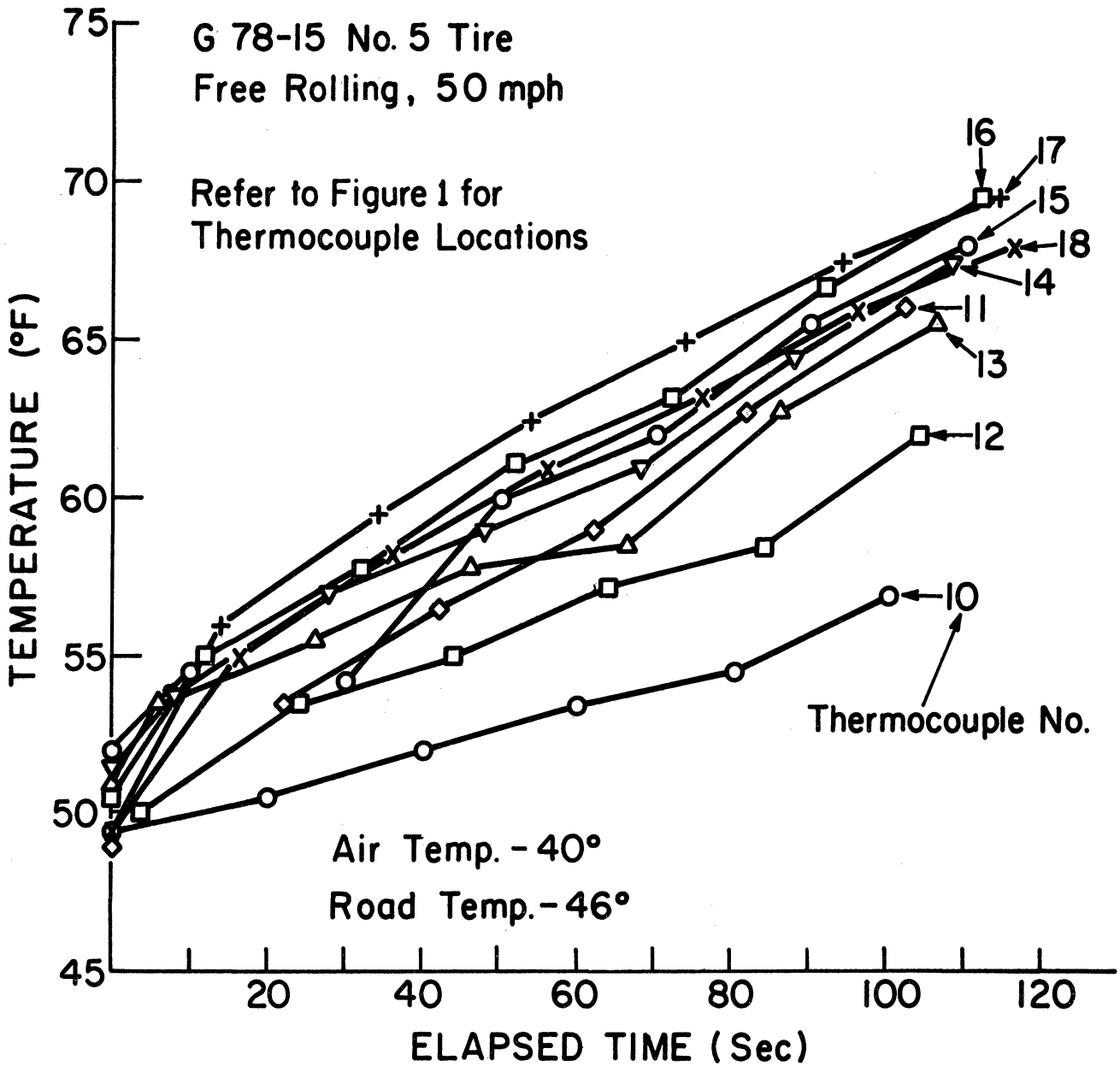

Figure 4. Temperature build-up within crown.

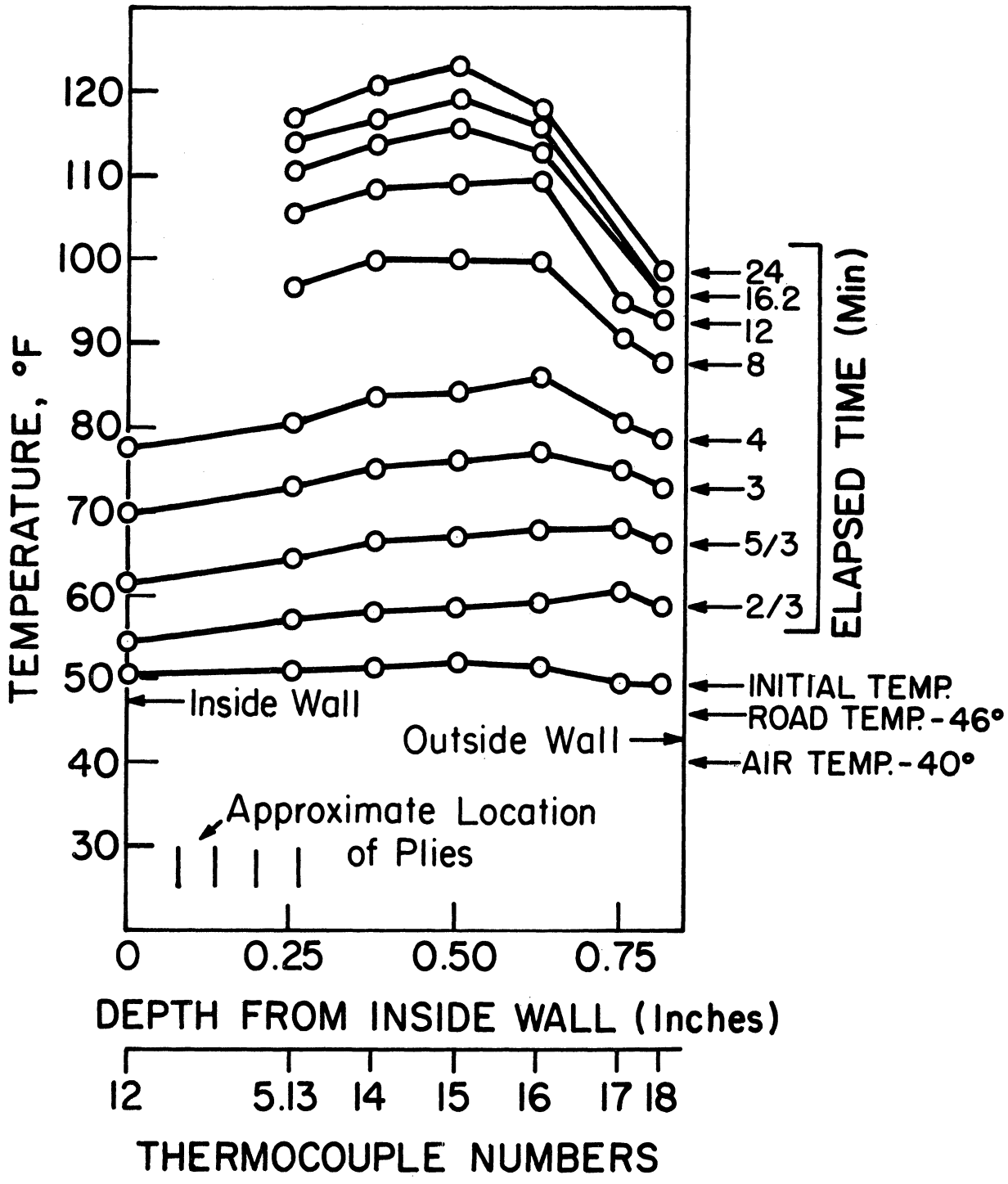

Figure 5. Temperature profiles at crown.

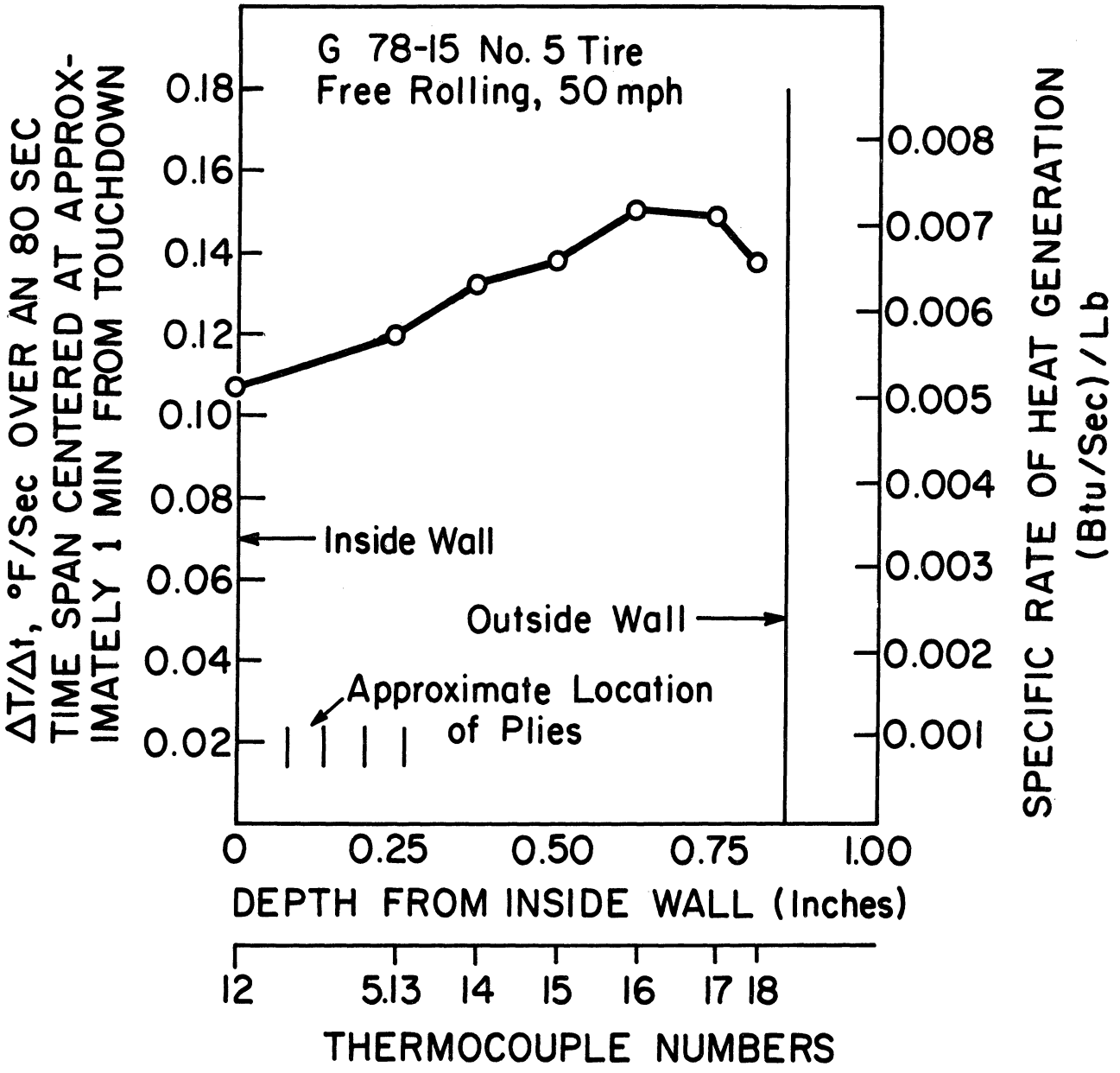

Figure 6. Heat generation profile at crown.

IV. TEMPERATURE SENSOR MEASUREMENTS

The purpose of the experiment is to measure the heat flux, if any, caused by the scrubbing of the tire and the road in the contact patch area. It is believed that the presence of very small sensors bonded to the road does not change the geometry of the deformation of the tire in the contact patch region. Therefore the heat flux measured by the sensor is due to scrubbing of the tire on the polyimide surface of the sensor. This heat flux and the heat flux between tire and road are proportional to the respective friction coefficients, tire-to-sensor and tire-to-road.

The experiment was performed on an asphalt taxiway at Willow Run Airport, Ypsilanti, Michigan.

The sensors used for these measurements were thin film nickel resistors sold under the designation type ETG-50B by Micro-Measurements, Inc., Romulus, Michigan. Their measuring area is 1/8 in. x 1/8 in., and their thickness approximately .001 in. Four sensors were bonded to the road with a thin layer of epoxy cement. The sensors used are made of a thin film of nickel between two layers of polyimide. The film is practically insensitive to strain but very sensitive to temperature. Figure 7 shows the dimensions and geometry of these sensors.

Figure 8 shows the sensor bonded to the asphalt road. Figure 9 shows the four sensors in place. On that figure notice:

(a) the white arrow indicating the direction of travel of the tire over the sensors,

(b) the four sensors 2.5 in. apart,

(c) the crack of the runway in which all wires are glued, and

(d) the triggering mechanism for the oscilloscope.

Each sensor was part of a bridge circuit shown in Figure 10. The sensitivity was found experimentally to be 0.77 mV/°F for E = 1.500 V and e_o = 0.00 at 75°F. A constant voltage power supply was used.

Two sensors at a time were used. Figure 11 shows the complete circuit. Figure 12 shows the trigger and zero balancing circuit.

A G78-15 patternless tire was used for the experiment, with inflation pressure of 24 psi and load of 1000 lb. The tire was mounted on the Highway Safety Research Institude truck and was in straight ahead free rolling position (see Figure 7). The tire was run at 50 mph and dropped on the road at fixed distances from the sensors. A device was put on the road in order to check the lateral position of the tire when passing over the sensors.

Numerous tests were run between June 1 and July 27 in order to determine the best experimental conditions. Sensitivity of the sensors to sun radiation necessitated the running of the experiment very early in the morning of a cloudy day.

The results of these tests are as follows:

(1) When the tire was dropped as close as possible to the sensors (bouncing of the tire limited this distance to a minimum of 100 ft) with an initial temperature equal to the temperature of the road, as appreciable heat flux could be detected.

(2) When the tire was rolled for a fixed distance of 1 to 2 miles before passing over the sensors, it was possible to pick up the surface temperature of the tire which was apparently due to heat build-up caused by hysteresis inside the tire.

(3) It is not feasible to run the tire under braking or yawed conditions because of the difficulty of dropping the tire at a distance less than a circumference before the sensors, and then the heat pulse measured is a combination of surface temperature and friction heat.

Two typical trials are shown:

(1) Trial 6 shows a slight cooling effect due to our initial temperature of the tire slightly less than the road temperature.

(2) Trial 8 shows the typical data when the tire has been run for 1 mile before passing over the sensors.

The computer program given subsequently in this section relates the temperature observed in the nickel film to the heat flux at the outer surface of the sensor. Prints of the contact patch show a length of 5.5 in. and a total area of 29.6 in.^{2}. Therefore the time of contact of the tire with the sensor is:

$$t = \frac{L}{V} = \frac{5.5 \times 3600}{50 \times 5280 \times 12} = 0.00625 \text{ sec}$$

The computer program is run for a unit heat flux pulse at the outer surface of the sensor for a duration of 6.25×10^{-3} sec and with the thermal

DATA FORM 036390

TRIAL NO. 6

OVERALL SENSITIVITY

.26 °F/cm

SENSOR # 2

SENSOR # 3

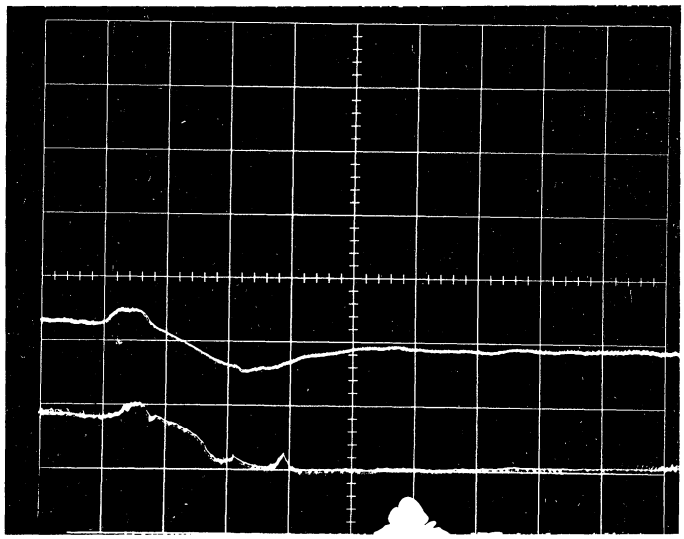

2 ms/cm SWEEP RATE

INSTRUMENTATION: ATTEN X _____ SCOPE SENS .2 mV/cm

VELOCITY 50 mph

TIRE: I. D. G 78-15 #5

LOAD 1000 lb PRESSURE 24 psi

TEMPERATURES °F

AIR 67

ROAD 75

TIRE 74

NOTES:

All speeds so far: 50 mph

DATA FORM 036390

Duration of contact based on contact patch length and velocity.

TRIAL NO. 8

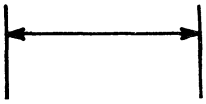

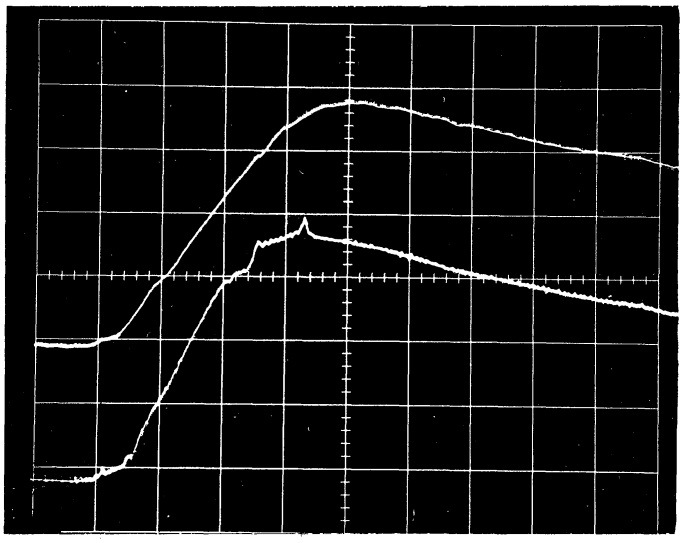

OVERALL SENSITIVITY

.26 °F/cm

SENSOR # 2

SENSOR # 3

2 ms/cm SWEEP RATE

INSTRUMENTATION ATTEN X ——— SCOPE SENS ———mV/cm

VELOCITY 50 mph

TIRE: I. D. 678-15 #5

LOAD 1000 lb PRESSURE 24 psi

TEMPERATURES °F

AIR 69C Bench 68TC

ROAD 77 TC

TIRE 84 TC

NOTES:

Tire down for / as in trial 8

characteristics of polyimide and asphalt. The thermal characteristics of asphalt were calculated from the composition furnished by the builder of the asphalt taxiway used in the experiment. A graph and table of the computer program are shown in Figure 14. The maximum ratio of temperature to flux is found to be 0.622×10^{-3} °F-ft^2-hr/Btu.

From the results of the experiments it was found that no increase in temperature could be found. As a way of checking, it is assumed that a 0. °F increase could be found, and calculations are conducted to find out what this increase would represent in terms of drag losses:

we have $\theta/q = 0.622 \times 10^{-3}$ °F-ft^2-hr/Btu and $\theta = 0.5$°F

therefore $q = 0.80 \times 10^{3}$ Btu/ft^2-hr

q corresponds to the part of F_o (total heat flux generated at the interface of tire and sensor) flowing into the polyimide. We have therefore

$q + q_r = F_o$ $\quad k_1, \alpha_1$ conductivity and diffusivity

and $q \dfrac{\sqrt{\alpha_1}}{k_1} = q_r \dfrac{\sqrt{\alpha_r}}{k_r}$

$$F_o = \left[1 + \sqrt{\frac{\alpha_1}{\alpha_r}} \frac{k_r}{k_1}\right] q = \left[1 + \sqrt{\frac{3.87 \times 10^{-3}}{4.46 \times 10^{-3}}} \frac{.16}{.0895}\right]$$

$$.80 \times 10^{3} = 2.13 \times 10^{3} \text{ Btu/ft}^2\text{-hr}$$

Therefore Q of friction between asphalt and rubber is $Q = F_o \times \dfrac{f_{asphalt}}{f_{polyimide}}$

f_{asph}: coefficient of friction between asphalt and rubber

f_{poly}: coefficient of friction between polyimide and rubber

The measured coefficients of friction were found to be

$$f_{as} = 0.80, \quad f_{pol} = 0.64$$

$$Q = 2.13 \times 10^{-3} \times \frac{0.80}{0.64} = 2.66 \times 10^{3} \text{ Btu/ft}^2\text{-hr}$$

But the contact patch area is 29.6 in.^{2}, therefore the heat due to friction is

$$D = \frac{2.66 \times 10^{3} \times 29.6}{144 \times 3600} = 0.152 \text{ Btu/sec}$$

And for a total drag of 25 lbf at 50 mph, the power loss in the tire is

$$\frac{25 \times 50 \times 5280}{778 \times 3600} = 2.32 \text{ Btu/sec}$$

and D is 6% of total drag loss

We see from our experiments and calculations that the friction heat generated at the interface of road and tire is a very small percentage of the total losses of the tire. Therefore all losses have to occur within the tire itself as hysteresis losses.

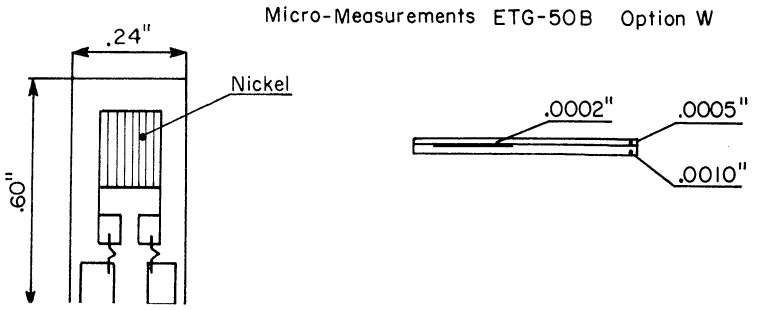

Figure 7. Detail of sensor construction.

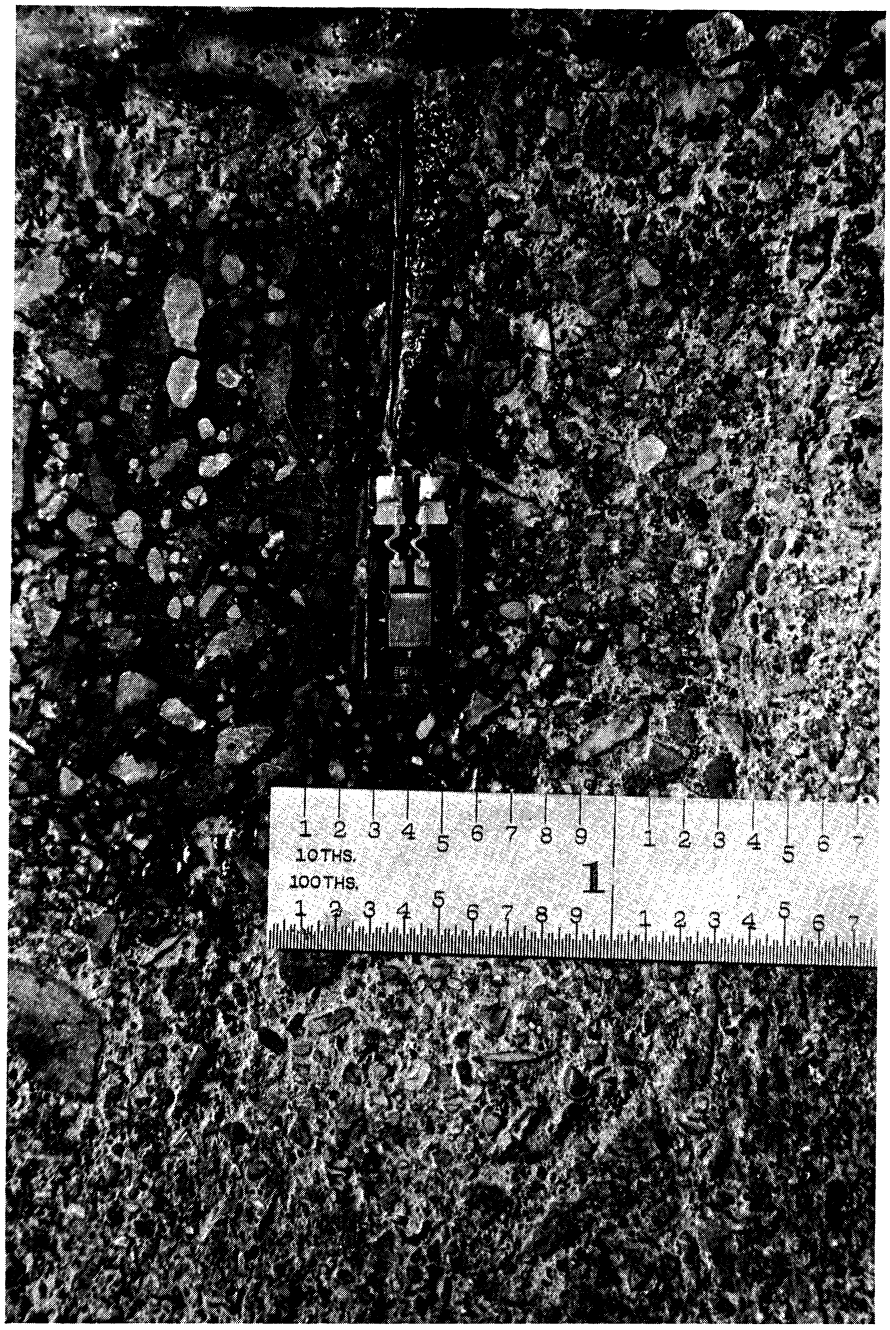

Figure 8. Sensor mounted on pavement.

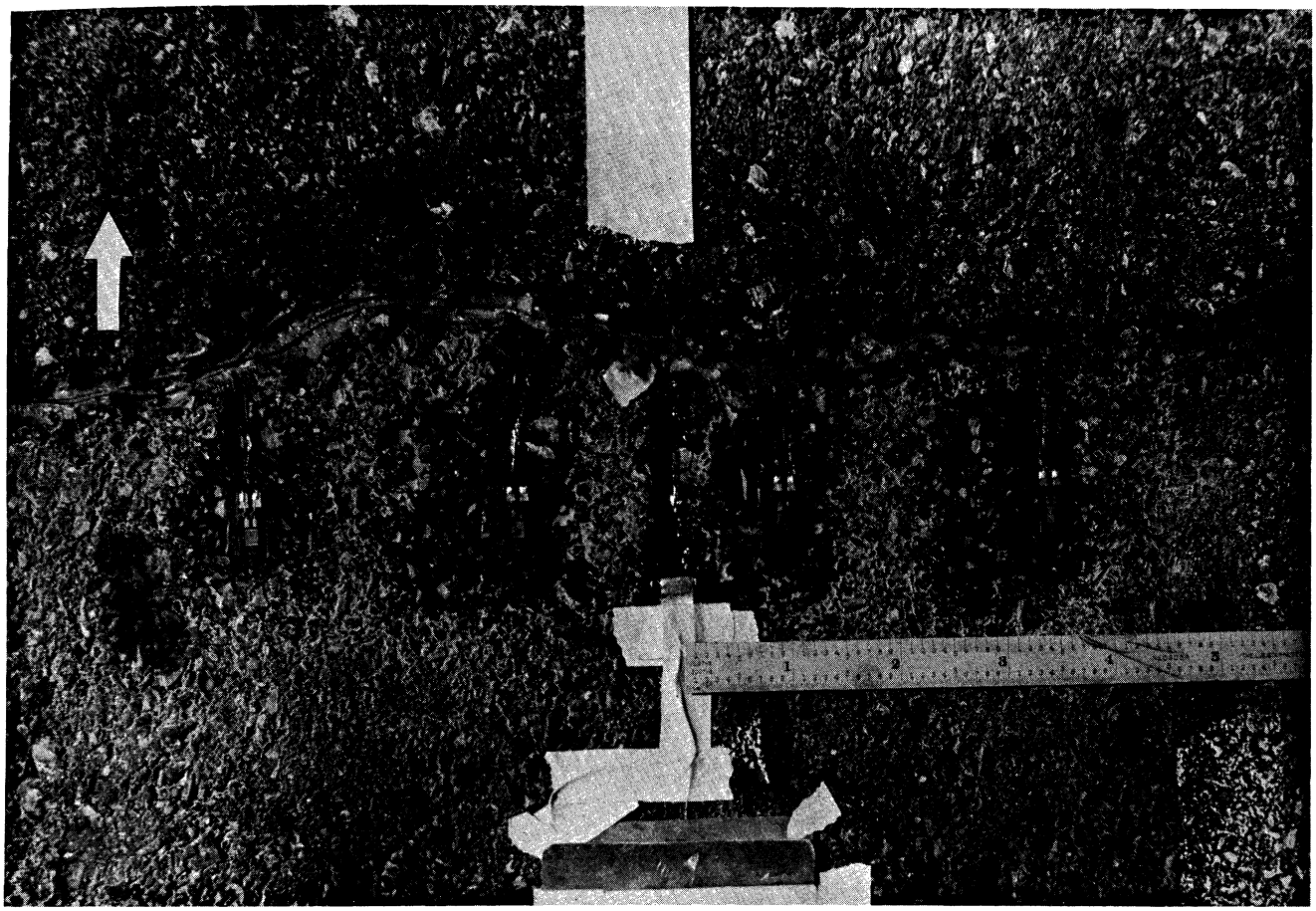

Figure 9. Sensor array on pavement. Trigger is located at end of rule.

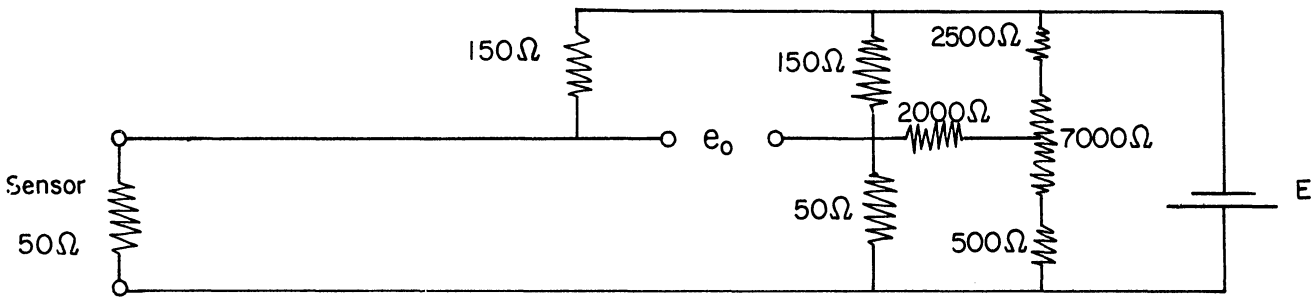

Figure 10. Bridge circuit for sensor.

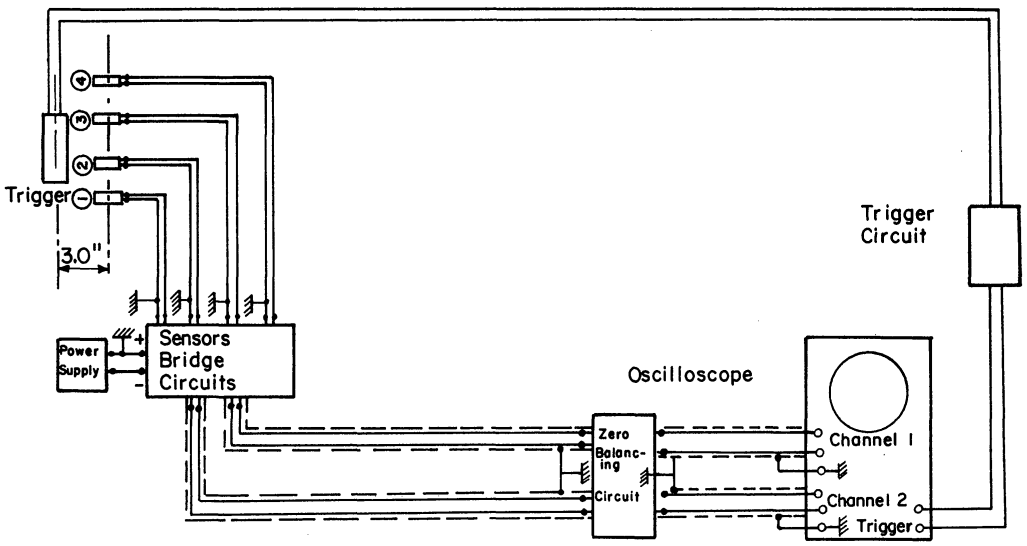

Figure 11. Schematic instrumentation for experiment.

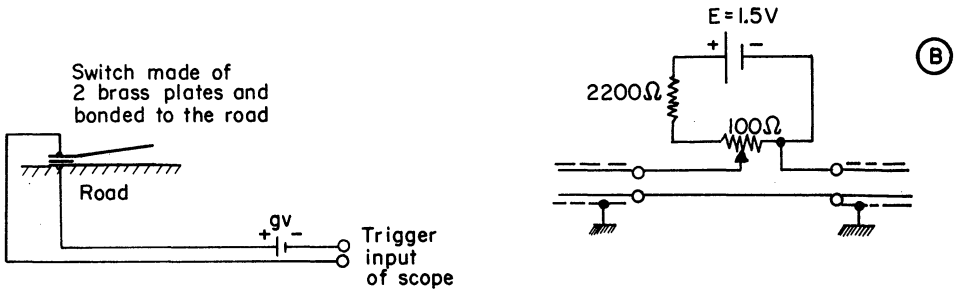

Figure 12. Trigger circuit and balancing circuit.

Figure 13. Treadless test tire mounted on truck.

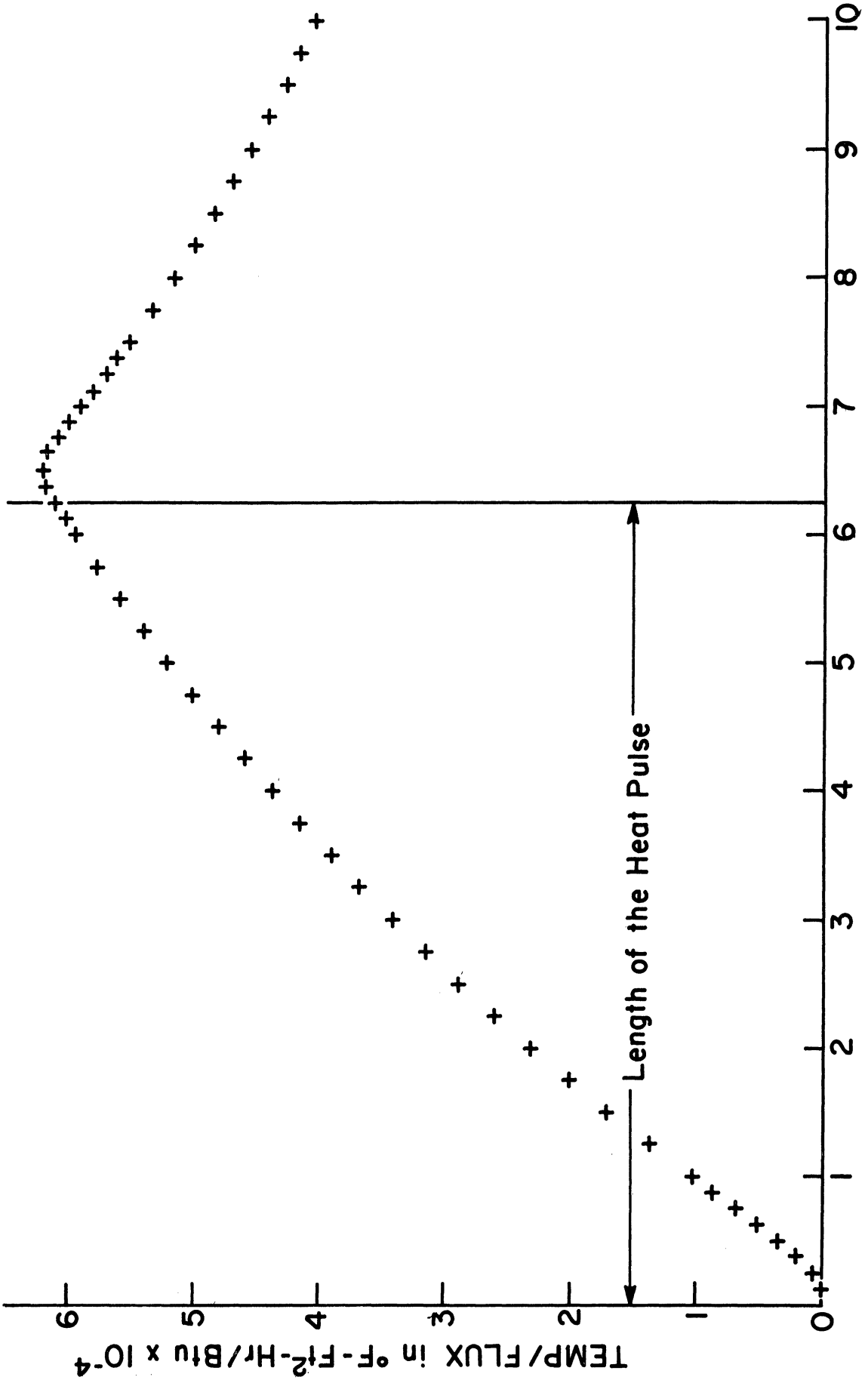

Figure 14. Temperature/flux as a function of time.

FIRST MATERIAL: CON1 ALP1 THICKNESS
0.8950E-01 0.3870E-02 0.1250E-03
SECND MATERIAL: CON2 ALP2
0.5600E 00 0.1760E-01
POSITION OF NICKEL/INTERFACE= 0.8333E-04 ASPHALT

SHAPE OF HEAT FLUX

TIME	MAGNITUDE
6.250	0.100000E 01

TABLE OF TEMPERATURE OVER FLUX

TIME IN MSEC	TEMP/FLUX IN NICKEL °F FT^2 HR/BTU	TEMP/FLUX AT SURF °F FT^2 HR/BTU
0.125	0.644466E-06	0.146147E-03
0.250	0.744536E-05	0.205684E-03
0.375	0.200160E-04	0.253135E-03
0.500	0.354733E-04	0.292295E-03
0.625	0.522452E-04	0.326786E-03
0.750	0.695470E-04	0.357887E-03
0.875	0.869749E-04	0.386670E-03
1.000	0.104315E-03	0.413367E-03
1.125	0.121451E-03	0.438442E-03
1.250	0.138321E-03	0.462159E-03
1.375	0.154894E-03	0.484716E-03
1.500	0.171155E-03	0.506268E-03
1.625	0.187101E-03	0.526939E-03
1.750	0.202732E-03	0.546827E-03
1.875	0.218053E-03	0.566014E-03
2.000	0.233072E-03	0.584567E-03
2.125	0.247787E-03	0.602543D-03
2.250	0.262234E-03	0.619990E-03
2.375	0.276394E-03	0.636950E-03
2.500	0.290284E-03	0.653457E-03
2.625	0.303912E-03	0.669543E-03
2.750	0.317288E-03	0.685234E-03
2.875	0.330417E-03	0.700554E-03
3.000	0.343308E-03	0.715523E-03
3.125	0.355967E-03	0.730161E-03
3.250	0.368402E-03	0.744484E-03
3.375	0.380619E-03	0.758506E-03
3.500	0.392624E-03	0.772241E-03
3.625	0.404424E-03	0.785702E-03
3.750	0.416023E-03	0.798900E-03
3.875	0.427428E-03	0.811844E-03
4.000	0.438644E-03	0.824545E-03
4.125	0.449676E-03	0.837011E-03
4.250	0.460528E-03	0.849251E-03
4.375	0.471206D-03	0.861272E-03
4.500	0.481714E-03	0.873081E-03
4.625	0.492056E-03	0.884685E-03
4.750	0.502237E-03	0.896090E-03
4.875	0.512261E-03	0.907302E-03
5.000	0.522131E-03	0.918327E-03
5.125	0.531851E-03	0.929170E-03
5.250	0.541426E-03	0.939837E-03
5.375	0.550857E-03	0.950332E-03
5.500	0.560150E-03	0.960659E-03
5.625	0.569307E-03	0.970824E-03
5.750	0.578331E-03	0.980831E-03
5.875	0.587225E-03	0.990683E-03
6.000	0.595993E-03	0.100038E-02
6.125	0.604637E-03	0.100994E-02
6.250	0.613161E-03	0.101935E-02
6.375	0.620921E-03	0.882476E-03
6.500	0.622410E-03	0.831076E-03
6.625	0.618016E-03	0.793629E-03
6.750	0.610624E-03	0.763342E-03
6.875	0.601811E-03	0.737589E-03
7.000	0.592361E-03	0.715021E-03
7.125	0.582682E-03	0.694840E-03
7.250	0.572990E-03	0.676527E-03
7.375	0.563403E-03	0.659720E-03
7.500	0.553994E-03	0.644160E-03
7.625	0.544768E-03	0.629643E-03
7.750	0.535771E-03	0.616033E-03
7.875	0.526998E-03	0.603194E-03
8.000	0.518451E-03	0.591035E-03
8.125	0.510125E-03	0.579475E-03
8.250	0.502017E-03	0.568451E-03
8.375	0.494120E-03	0.557906E-03
8.500	0.486427E-03	0.547786E-03
8.625	0.478931E-03	0.538080E-03
8.750	0.471627E-03	0.528726E-03
8.875	0.464506E-03	0.519705E-03
9.000	0.457564E-03	0.510991E-03
9.125	0.450792E-03	0.502563E-03
9.250	0.444187E-03	0.494402E-03
9.375	0.437741E-03	0.486490E-03
9.500	0.431448E-03	0.478814E-03
9.625	0.425308E-03	0.471359E-03
9.750	0.419310E-03	0.464114E-03
9.875	0.413452E-03	0.457068E-03
10.000	0.407728E-03	0.450210E-03

REMARK: UNIT OF TEMP/FLUX IS F-FT**2-HR/BTU
#EXECUTION TERMINATED

Figure 14. (Concluded)

V. SCRATCH PLATE MEASUREMENTS

One relatively simple mechanical method for measuring the energy losses at the surface of a rolling tire is to cause the loaded tire to roll over a smooth metallic plate upon which carborundum particles have been sprinkled. The grit embeds itself in the tread rubber and causes scratch marks on the plate surface as the grit particles pass through the tire contact patch. These scratch marks are indications of the amount of surface scrubbing present in the tire contact patch area.

It is difficult to assess the accuracy of this method. Insofar as is known there is no study presently available comparing the measured deflections obtained from scratch records with those obtained from more sophisticated instrumentation. It must be surmised that the scratch records could not, in general, be larger than the displacements undergone by the tire surface in the absence of the grit, provided that the friction coefficients between the actual road surface and the metallic plate were the same. This is because the embedding of the grit particles into the rubber surface would, in general, cause scratch records to be equal to, or smaller than, the actual distances moved. In view of the uncertainty between the actual distances and the resulting scratch records, and the additional uncertainties concerning equality of the friction coefficient between a real roadway and a metallic plate, these scratch records can only be used as an indication.

In the specific work reported here, 8.25 x 14 size bias belted passenger tires furnished without tread pattern by the B. F. Goodrich Tire Company were

used on The University of Michigan Highway Safety Research Institute flat plank tire testing machine in order to produce such scratch records. The plates used were .005-in. brass, and the grit material was carbotundum. The load on the tires was 1000 lb at an inflation pressure of 24 psi. These are standard conditions which have been used on these same tires for other tests.

The tires were rolled in straight line, nonbraking, fashion over the scratch plates in three separate tests. The scratch plates were observed under a medium power microscope and the length of the resulting scratches were measured. These lengths were averaged over the width of the contact area and the total length of scratch, on the average, was found to be 0.02 in.

Assuming a pressure distribution equal to the inflation pressure of 24 psi, assuming a contact patch width of 6 in., and further assuming a friction coefficient between the tire and brass plate of 0.8, a total drag force associated with these tires, due to surface scratching alone, can be computed. This gives a value of drag force due to surface scrubbing $\simeq$ 2.0 lb.

In view of the fact that other measurements indicate that the total drag force associated with these tires at slow speeds is at least 20 lb, then one must conclude from these scratch records that the surface effects cause a contribution to the total energy loss which is approximately 10% or less of the total. This means that only a very small portion of the total losses can be ascribed to surface scrubbing directly, at least at these low speeds.

VI. MODEL TIRE STUDIES

Two basic types of experiments were carried out on a 4.5 in. diameter tire, scaled down from a Type VII 40 x 12-14 PR aircraft tire. The tire model and its construction are described in Ref. [3]. One experiment was to measure the drag force of the free-rolling tire, while the other experiment was to measure the surface temperature of the free rolling tire. Both experiments were performed on a 30 in. diameter road wheel using two different surfaces of contact for the tire. One surface was the cast iron of the road-wheel itself, while the other surface was Safety Walk.* In a separate experiment these two surfaces exhibited similar static coefficients of friction. However, since the Safety Walk is made up of abrasive sand grains bonded by a glue to cloth backing, it is clear that their thermal properties are quite different. No formal attempt was made, however, to measure the thermal characteristics of the Safety Walk.

Drag-force measurements were made on the freely rolling tire by use of small force transducers located in the axle between the tire and its supporting yoke. At the same time the side force perpendicular to the wheel plane was measured as a function of yaw angle. Bearing drag was estimated and subtracted from the drag-force measurements by use of a Plexiglas model wheel of the same size as the tire, but of essentially rigid construction and with extremely low loss characteristics. By subtracting this bearing drag component, the actual tire drag could be obtained for any set of conditions.

*Trade Mark.

Tire surface temperatures were measured with an Ircon model CH-34L infrared radiation thermometer which has been previously calibrated for the emissivity of rubber. For these experiments, the average image size was approximately 3/16 in. in diameter so that the temperatures recorded represent averages over that area of the tire. Although a single individual operated this instrument throughout most of the experiments reported here, several people made check measurements from time-to-time to establish that there was no gross biasing in the temperature measurements. Figure 15 shows the location of the positions at which temperature was measured.

The procedure for recording drag forces and tire temperatures was kept constant throughout these experiments. Each test was begun with both tire and rim allowed to cool to equilibrium temperature before beginning the test. The tire was allowed to run 4 min at the first test speed (500 rpm) at which time data was taken for drag load and temperature. Each successive speed value was then run for 2 min before data was again recorded. This procedure was followed for all yaw angles, and under a vertical load of 38 lb and with a 20 psi inflation pressure for this particular model tire.

While considerable care was taken in measuring the steer angle values quoted in the subsequent figures, the mechanism for this was not as accurate as desired and so one must interpret the resulting yaw angle data as subject to an error of approximately ±1°.

Considerable care was also taken to insure that the measurements of temperature with the two different surface coatings on the roadwheel were taken under identical yaw angle conditions. This was accomplished by setting

the test tire at a particular yaw angle and carrying out the measurements of temperature on both surfaces without changing this yaw angle setting.

Figures 16, 17, and 18 are typical surface temperatures measured at the three basic positions on the tire for zero yaw angle. On all three figures, it will be noticed that for both surfaces on the roadwheel, the center tread position is the coolest, the sidewall is the hottest while the shoulder surface temperature is intermediate. As is to be expected, the temperatures and temperature differences at the three positions increase with speed. Figure 18 is particularly interesting in that it can be seen that both the center tread and shoulder positions exhibit higher temperatures while running on the Safety Walk surface than they do when running on the cast iron surface. However, the sidewall temperatures are the same for both roadwheel surfaces.

Figures 19 and 20 show the temperature change through the contact patch for the center tread and shoulder positions. Shoulder temperature is taken on the so called tension shoulder as shown in Figure 15. The tension shoulder temperature shows a definite tendency to increase on both road surfaces for both the 0° and 2° yaw angle conditions, but not for the other yaw angle conditions. There does not appear to be a great deal of speed dependence on this data. There is little strong evidence here that the tread either cools or heats in passing through the contact patch.

Unfortunately the arrangement of the experimental apparatus did not allow us to measure the temperature on the compression shoulder of the tire as it passed through the contact patch. Consequently, little can be concluded about this particular position on a yaw tire. Figure 21 shows temperature difference

between the compressed shoulder and the tension shoulder at the entrance to the contact patch of a yawed tire. On both roadway surfaces the compressed shoulder is hotter than the tension shoulder in general.

Figure 22 shows the temperature difference between the compression sidewall and the tension sidewall under identical running conditions. Here, the compressed sidewall is always hotter than the tension sidewall, with little influence of roadwheel surface apparent here.

Figures 23 through 28 illustrate particular temperature levels for various positions on the tire under different yaw angles and speeds, using the two different roadwheel surfaces. In general, study of this data leads one to the following conclusions:

(1) Temperatures increase in the tire with an increase in yaw angle.

(2) Temperatures increase in the tire with an increase in speed.

(3) Sidewall temperatures are independent of the roadwheel surface.

(4) Points on the tire coming into contact with the road surface are hotter when run on the Safety Walk than on the cast iron.

This latter point is quite clearly demonstrated in Figure 29, which shows the difference in temperature between the two surfaces for the center tread and tension shoulder positions.

Figures 30 and 31 illustrates drag force in the wheel plane and drag force in the direction of motion, respectively, as a function of speed at several yaw angles. The nonlinearity of the data with yaw angle probably indicates errors in the measurement of 0° yaw angle position, as previously mentioned. In examining this data, there appears to be little difference

between drag forces measured on the Safety Walk or cast iron, indicating minor effects from scrubbing contact. This is substantiated by Ref. [5].

Finally, it should be noted that examination of this data seems to indicate that the temperature difference between entering contact and leaving contact, as measured on the tread of the tire, seems to be approximately independent of the surface material upon which the tire runs, but to the best of these measurements is a very small quantity, thus not clearly substantiating the hypothesis of Schallamach concerning temperature rise in the contact region of the tire.

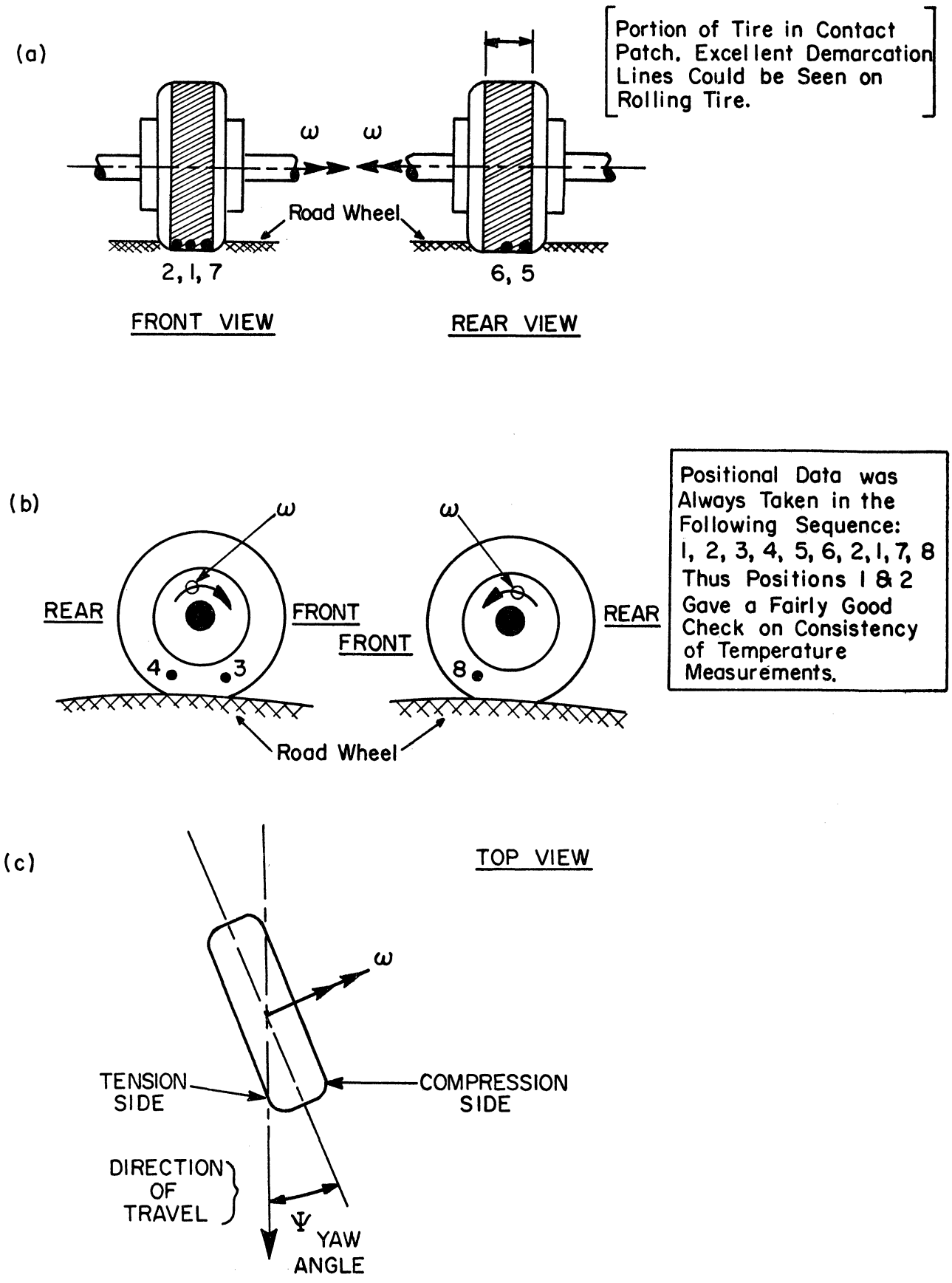

Figure 15. (a) and (b) Positional information for surface temperature measurements; (c) tire as viewed from top.

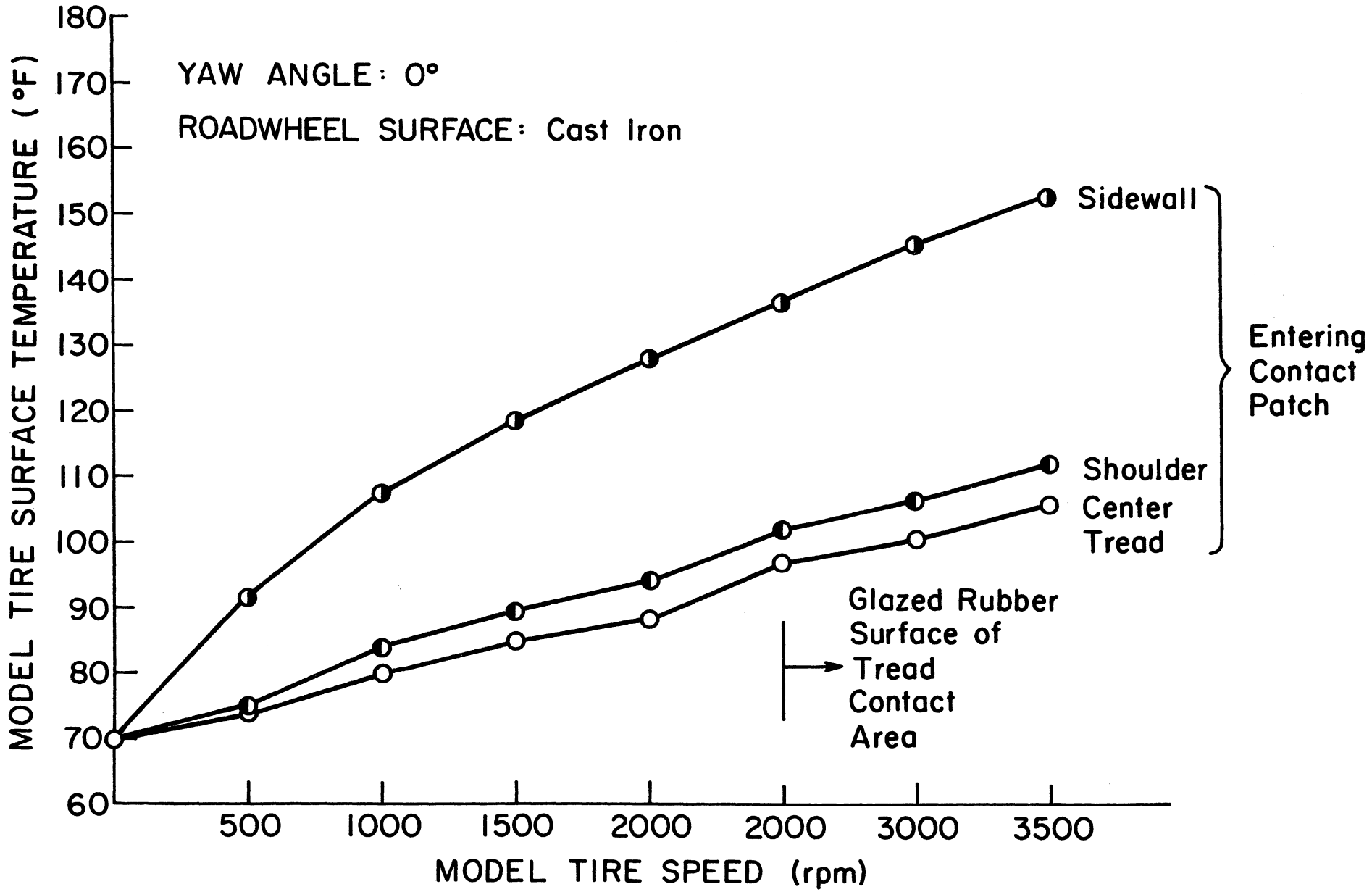

Figure 16. Surface temperatures at various positions vs. speed on cast iron at 0° yaw.

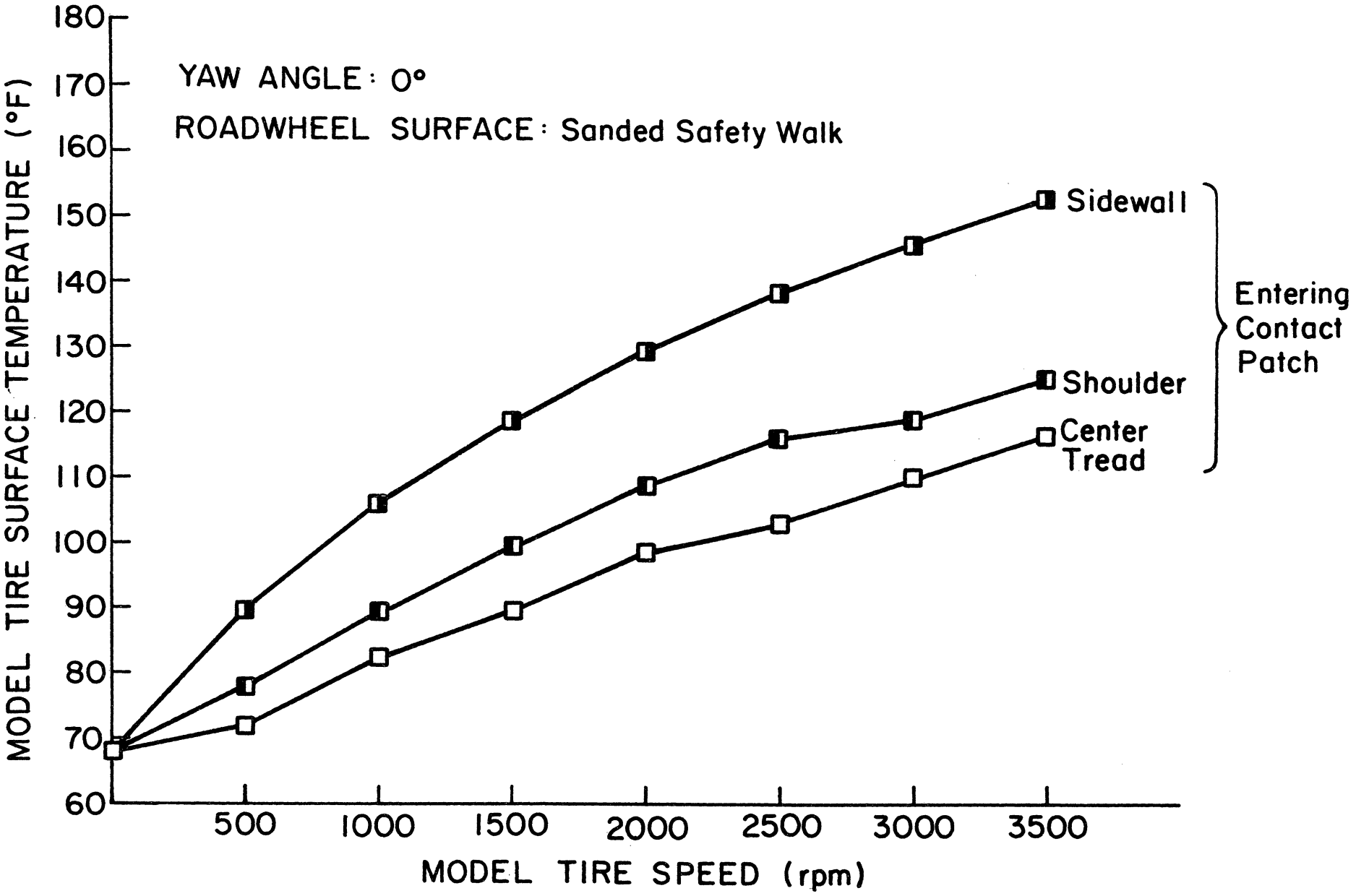

Figure 17. Surface temperatures at various positions vs. speed on sanded Safety Walk at 0° yaw.

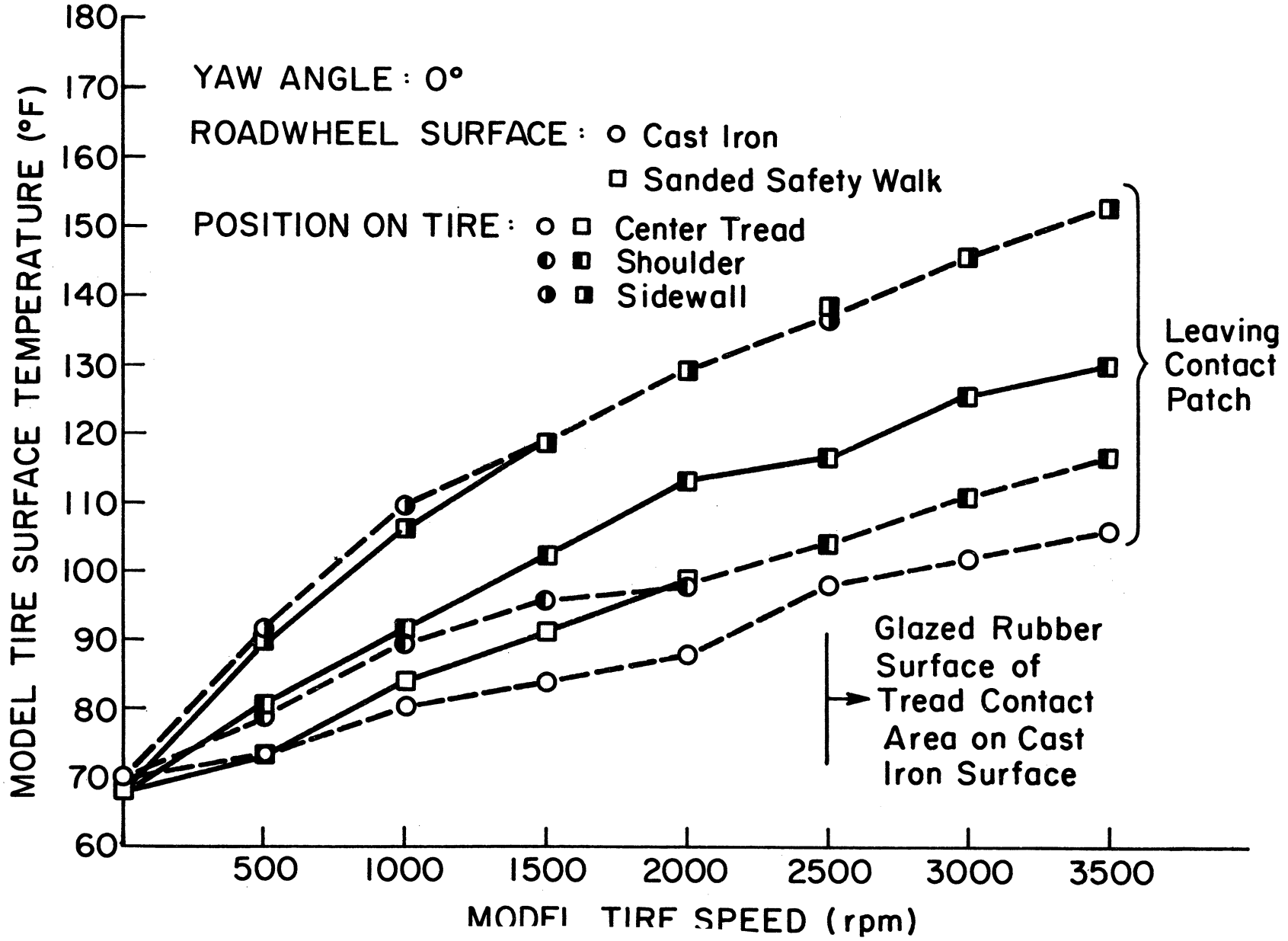

Figure 18. Surface temperatures at various positions vs. speed on cast iron and sanded Safety Walk at 0° yaw.

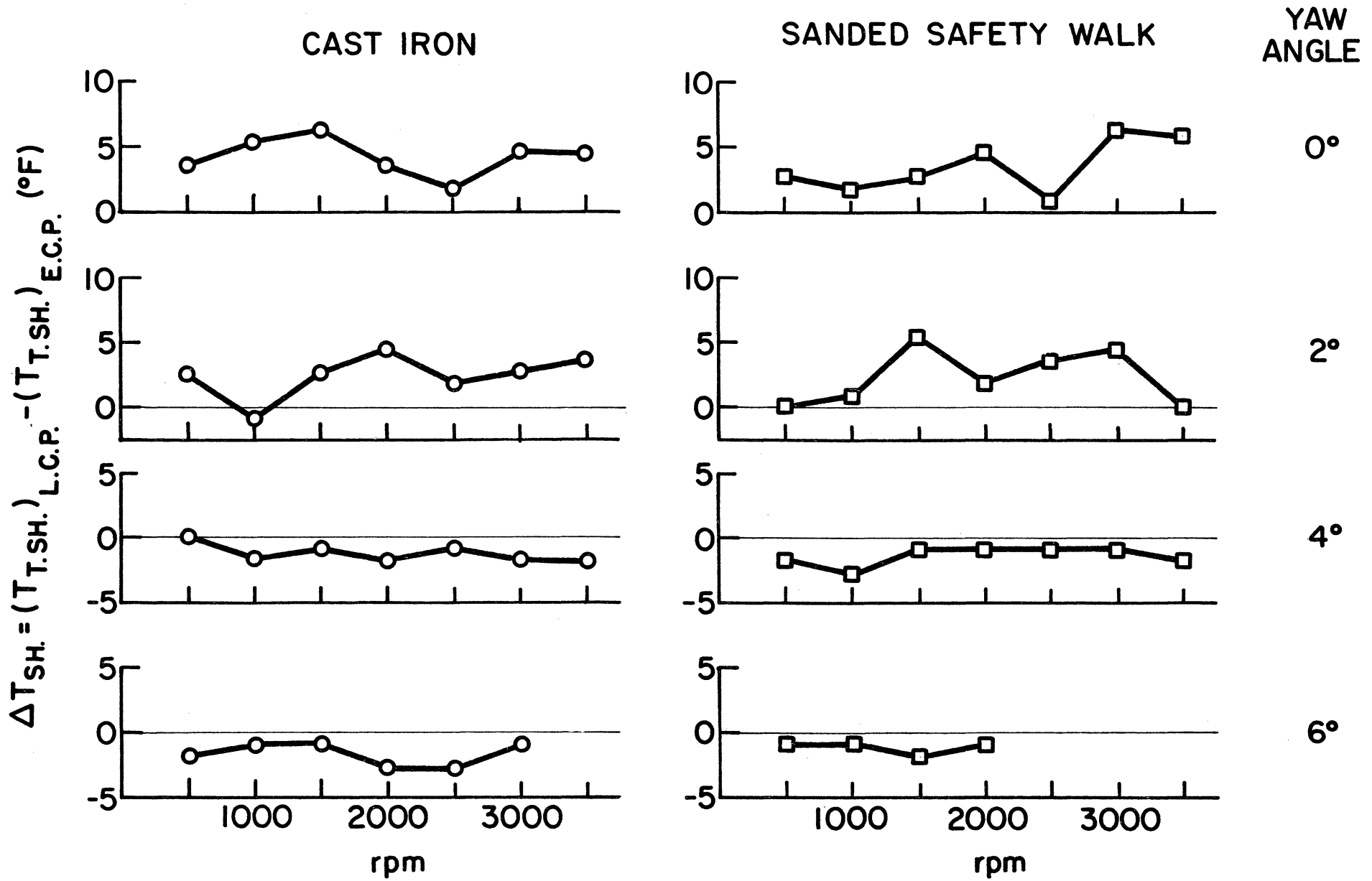

Figure 19. Temperature change of tension shoulder after going through contact patch vs. speed.

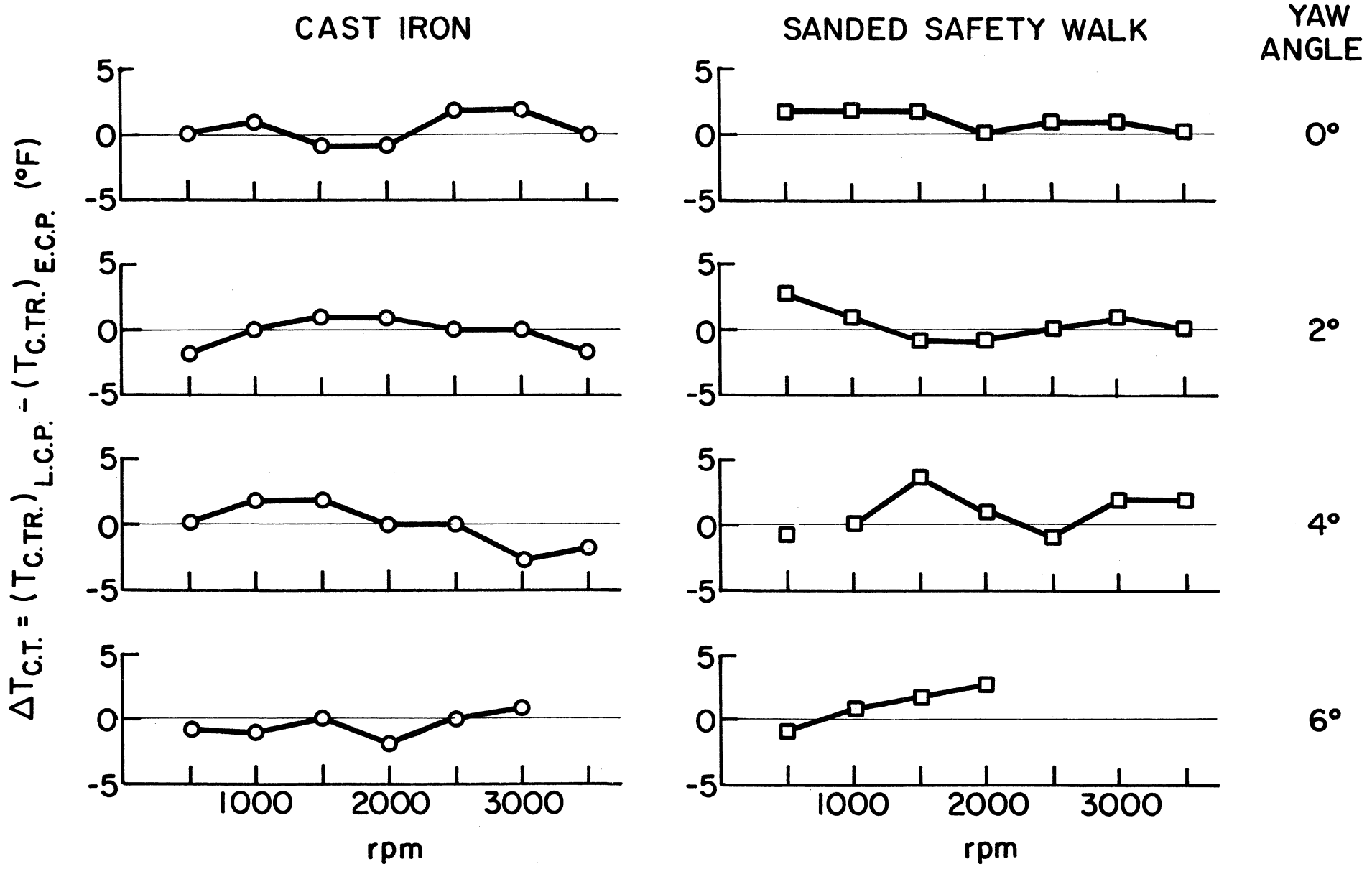

Figure 20. Temperature change of center tread after going through contact patch vs. speed.

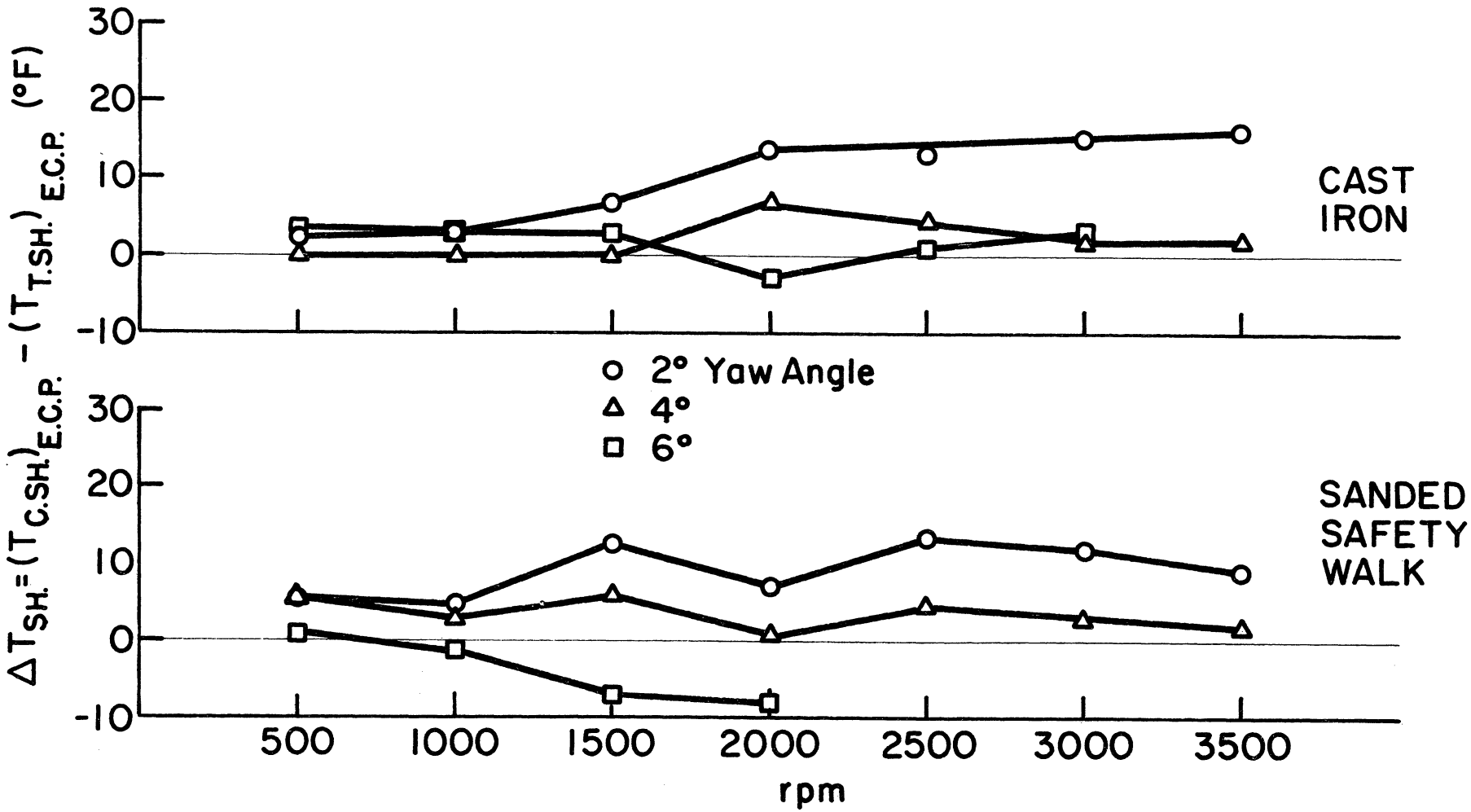

Figure 21. Temperature difference between compressed shoulder and tensioned shoulder vs. speed.

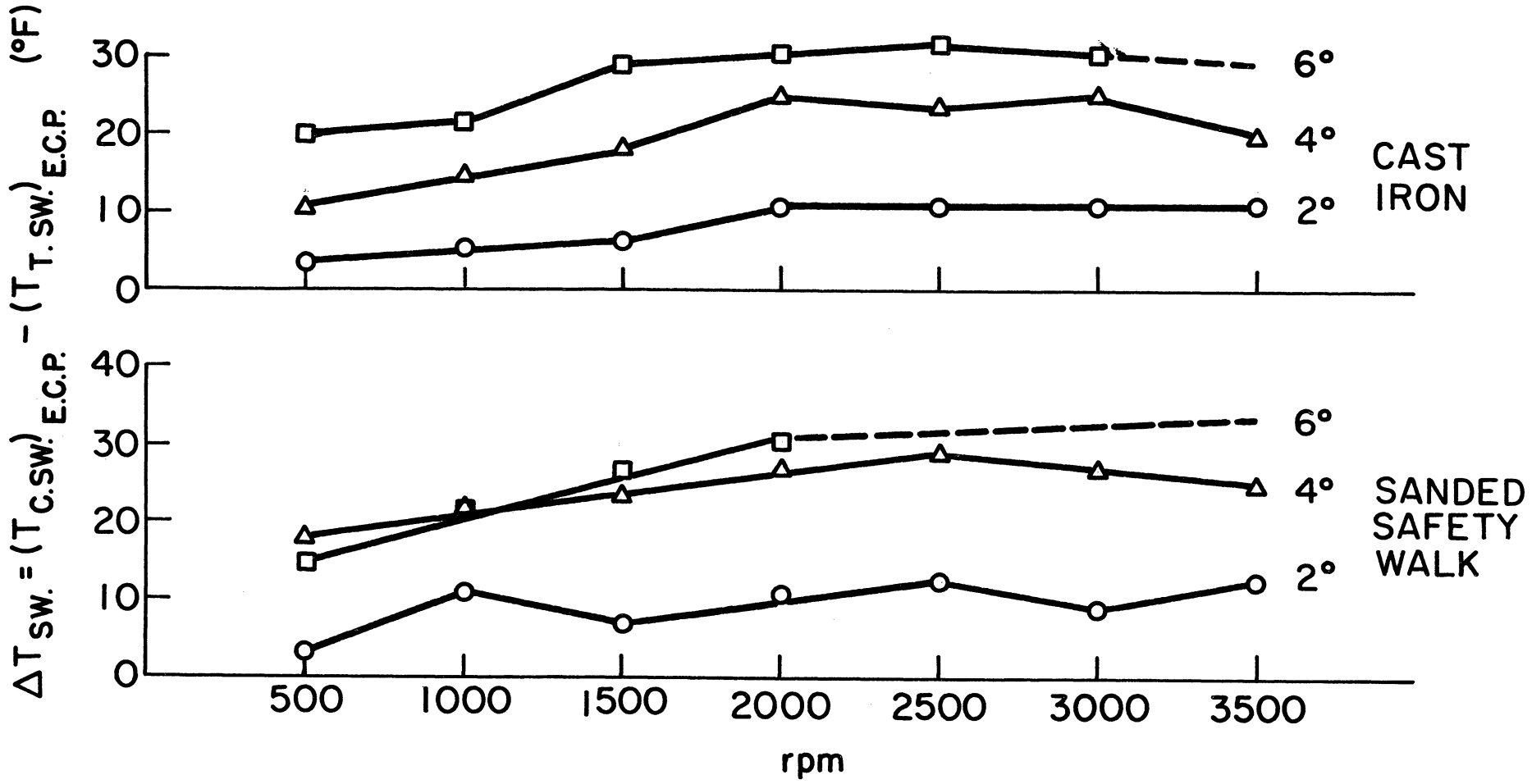

Figure 22. Temperature difference between compressed sidewall and tensioned sidewall vs. speed.

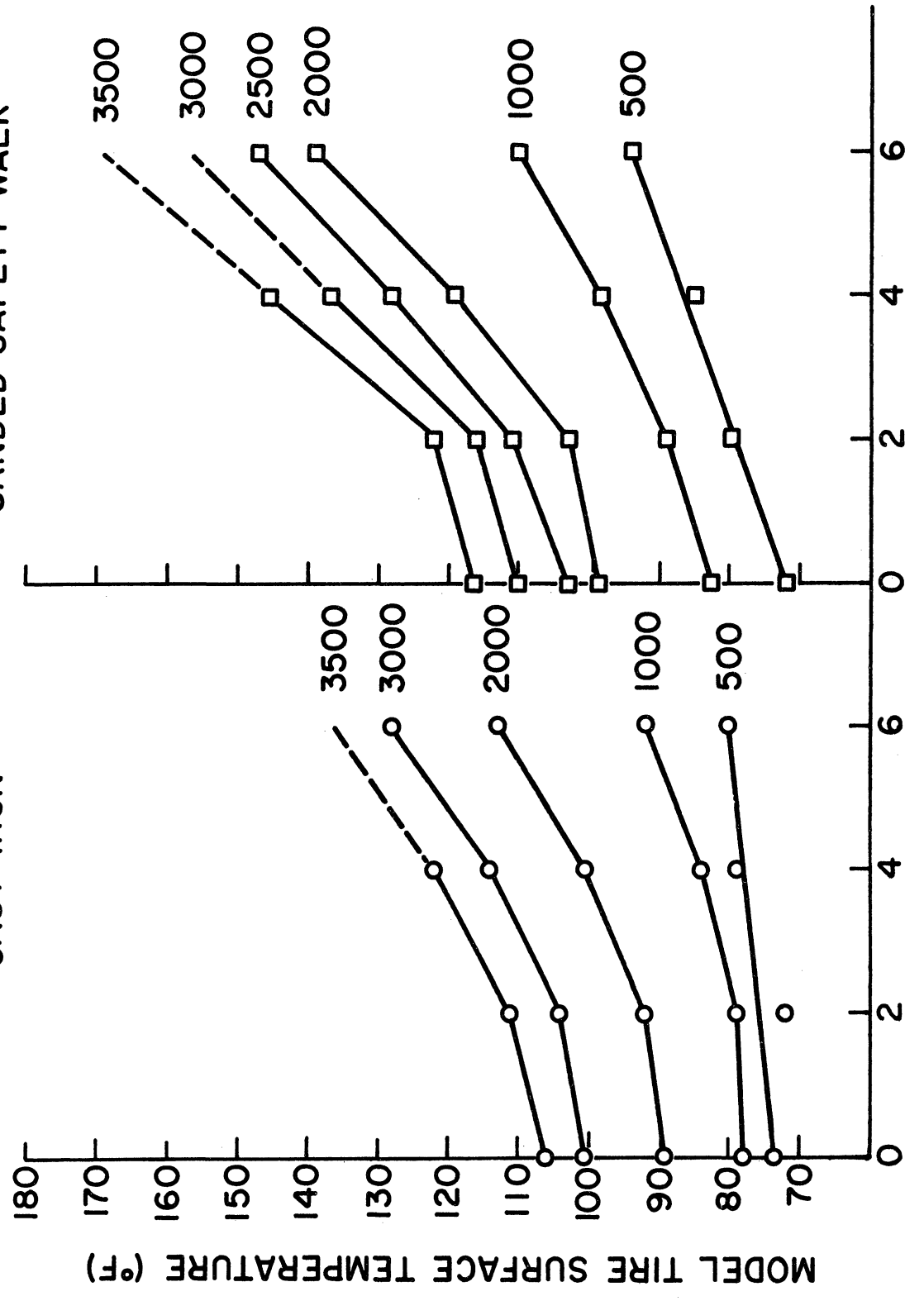

Figure 23. Center tread temperature entering contact patch.

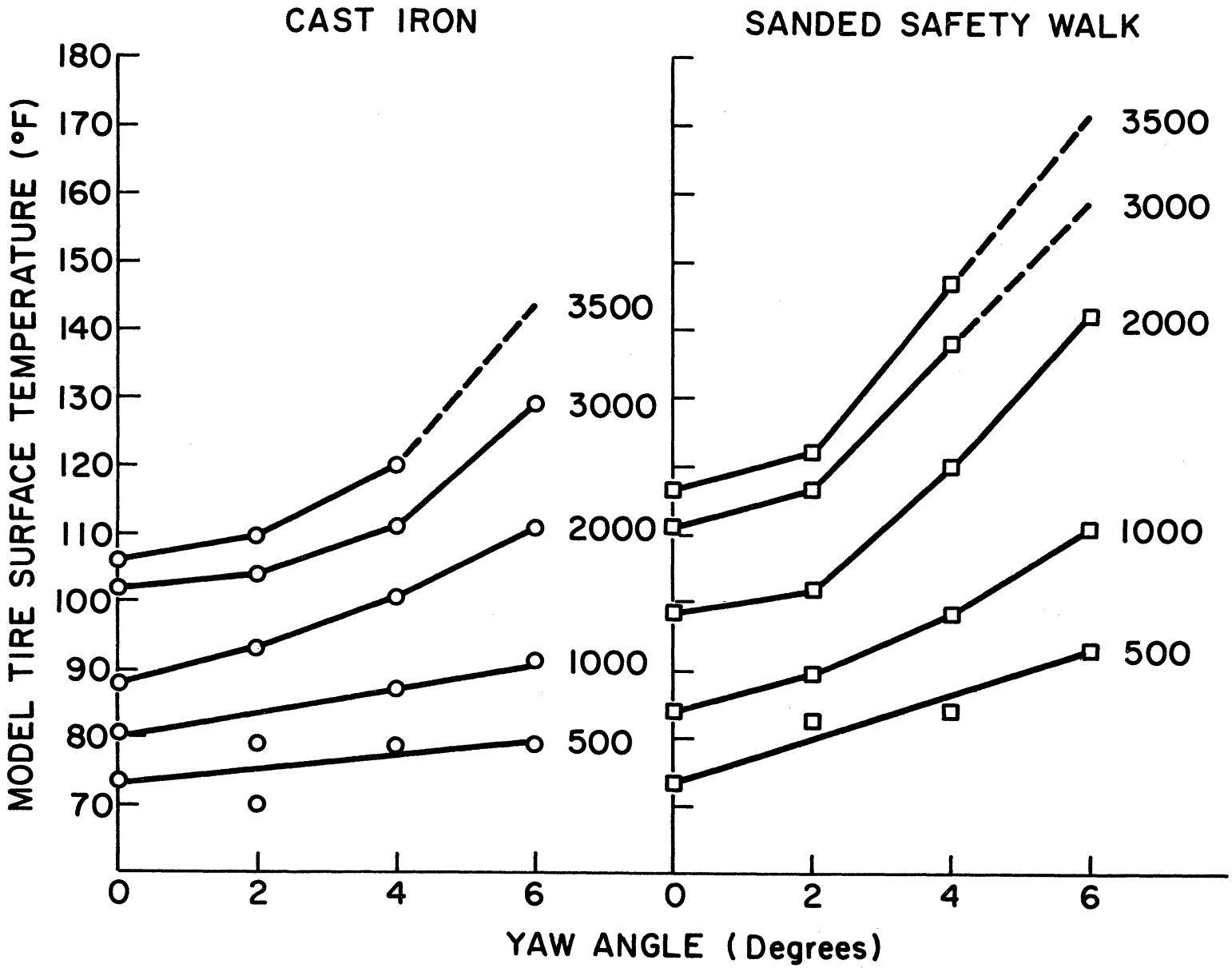

Figure 24. Center tread temperature leaving contact patch.

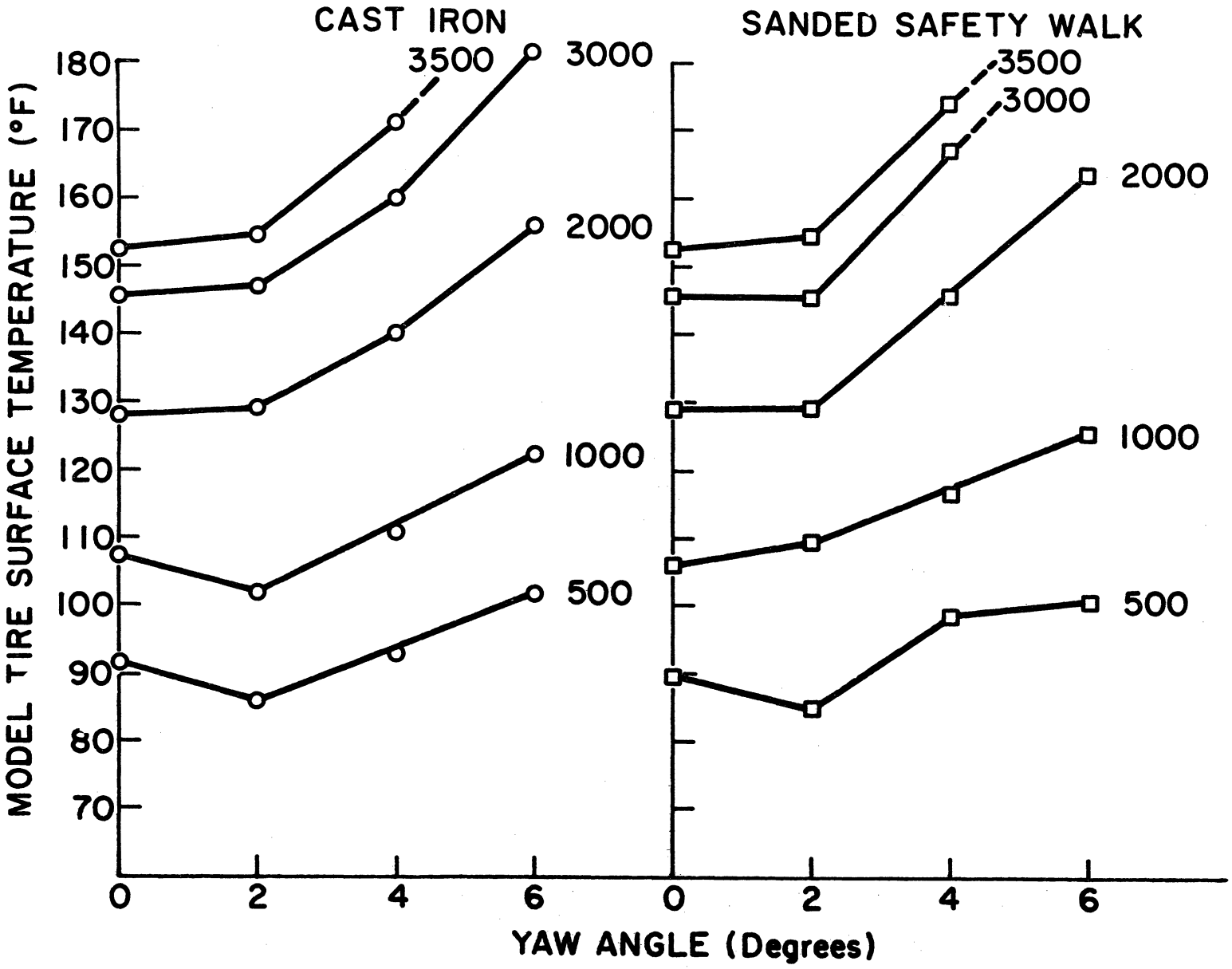

Figure 25. Compression sidewall temperature entering contact patch.

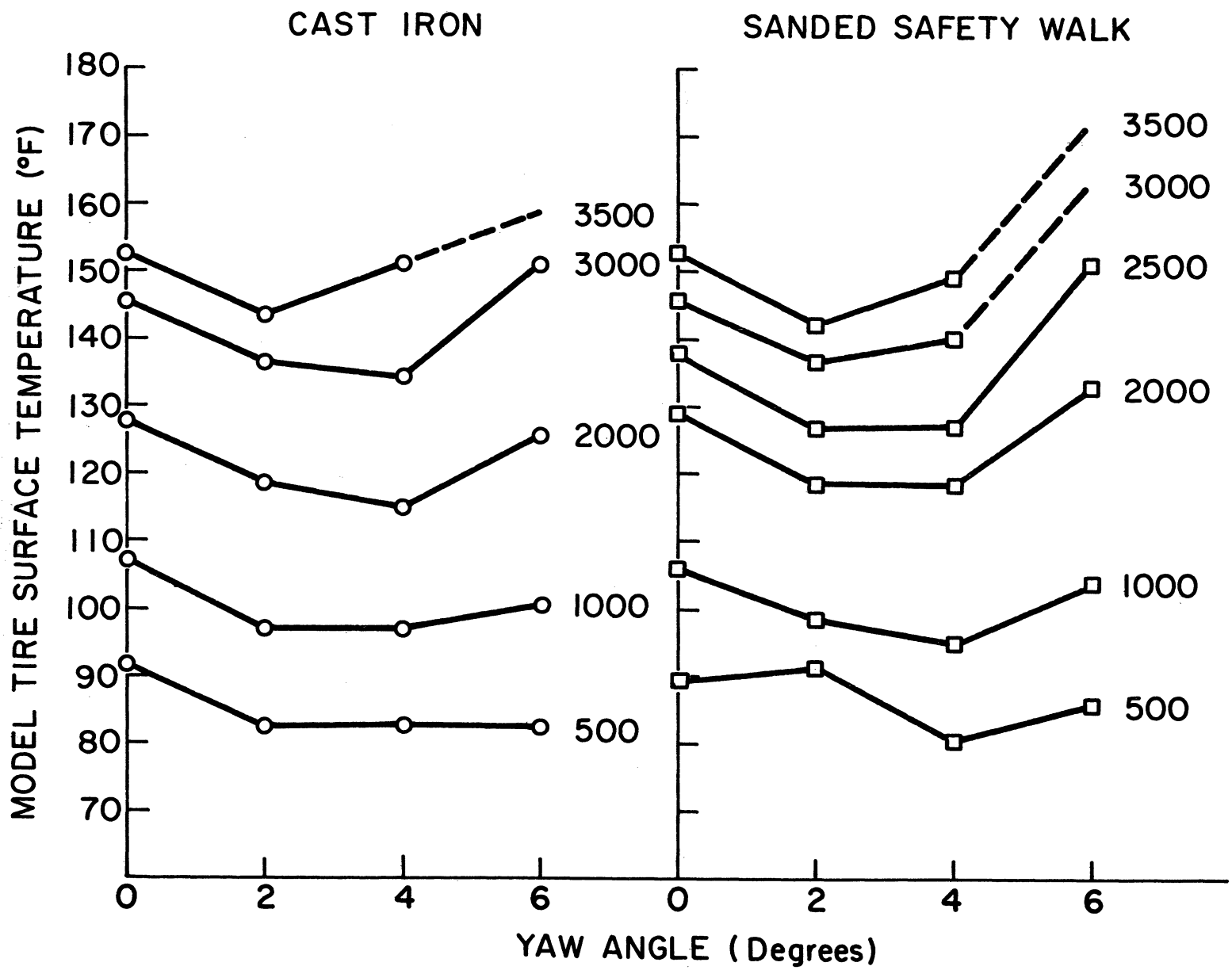

Figure 26. Tension sidewall temperature entering contact patch.

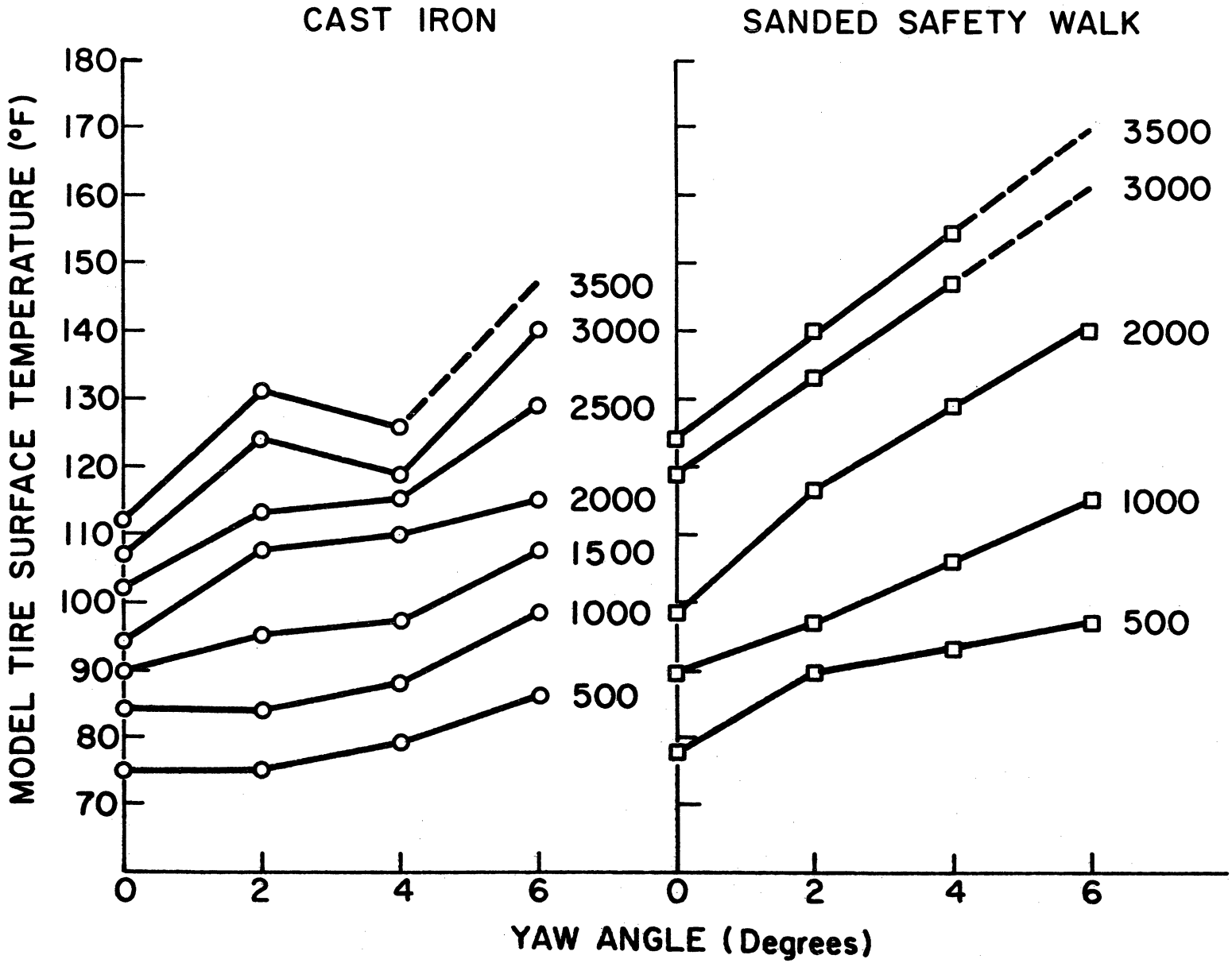

Figure 27. Compression shoulder temperature entering contact patch.

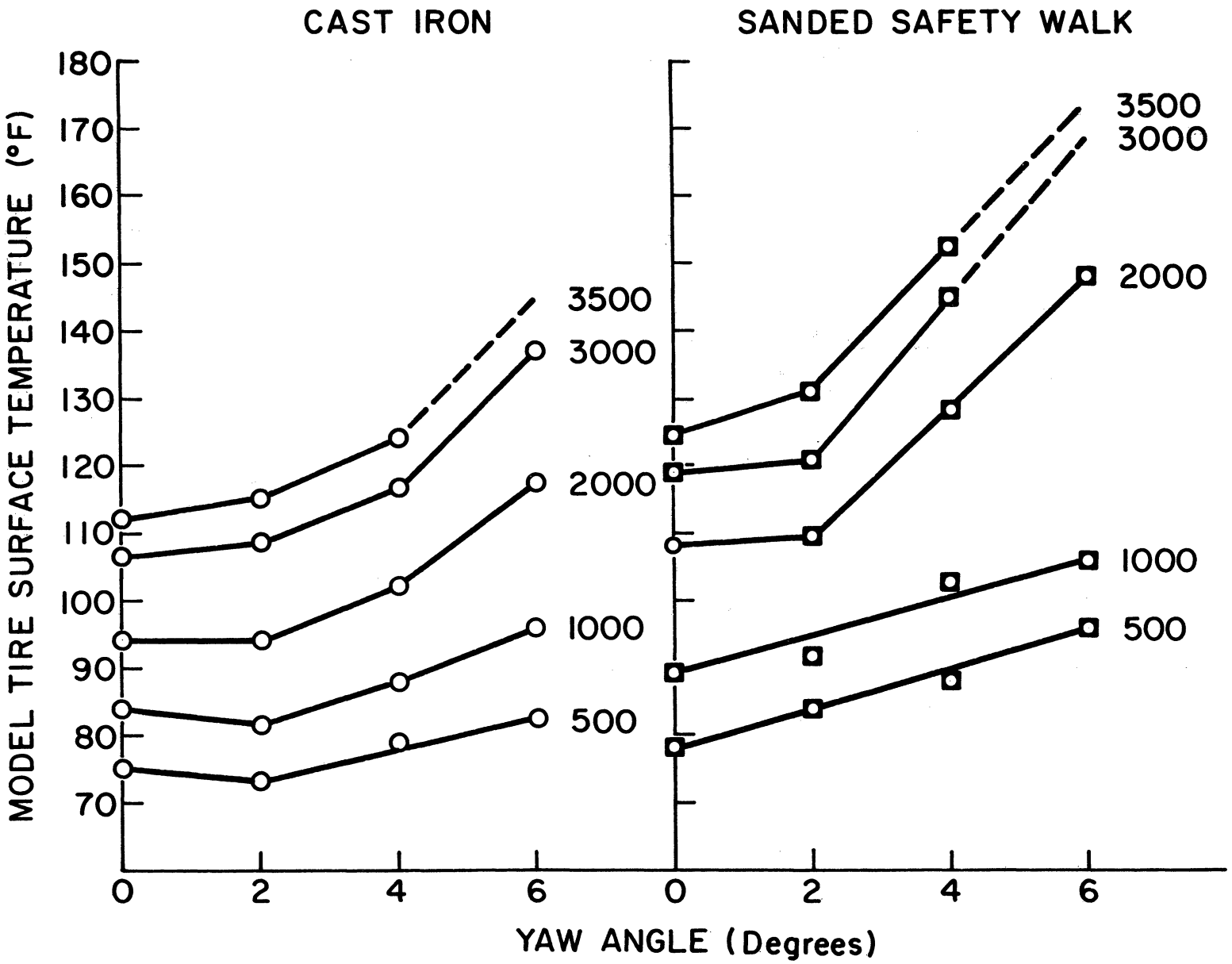

Figure 28. Tension shoulder temperature entering contact patch.

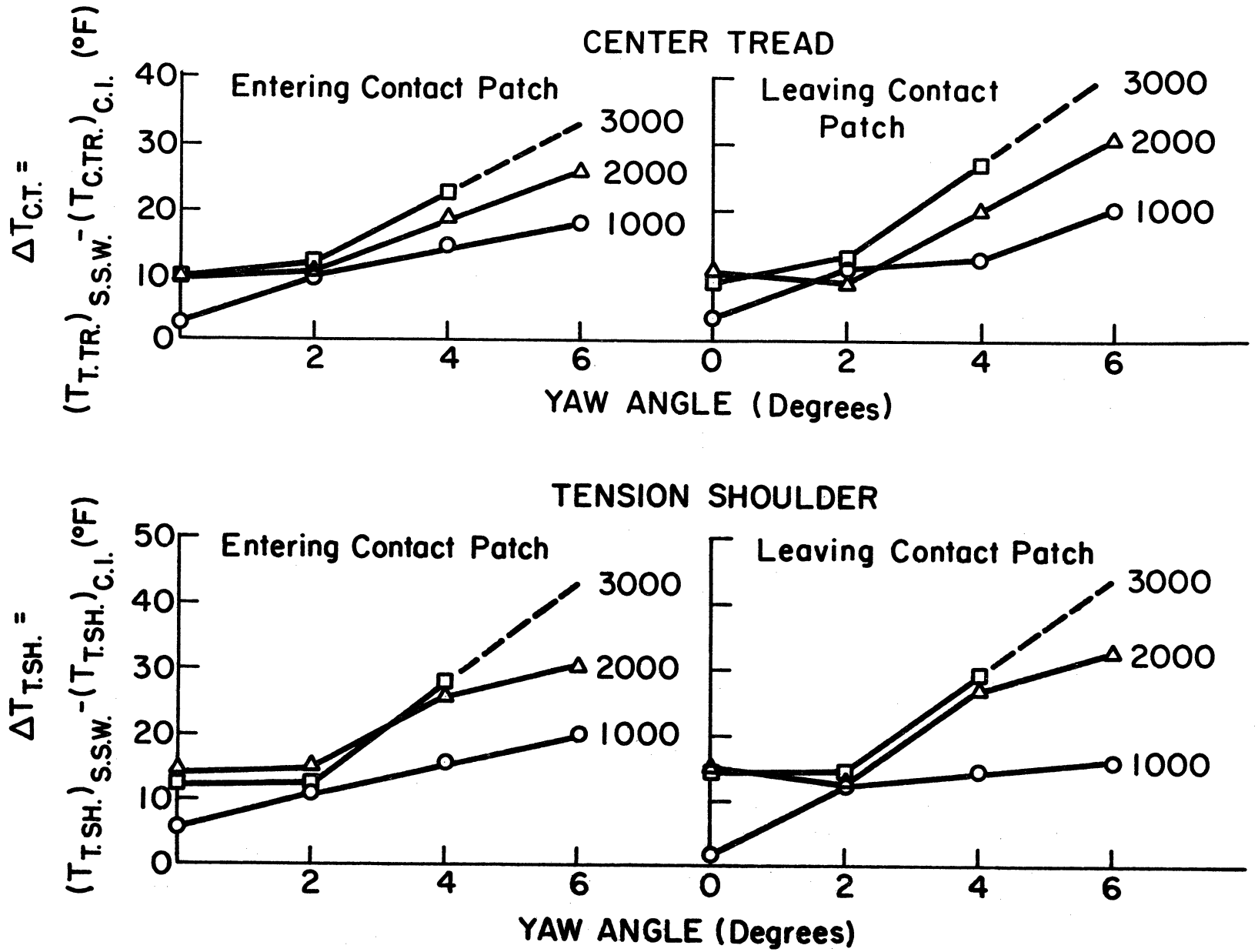

Figure 29. Temperature difference of center tread (and tension shoulder) between cast iron and sanded Safety Walk.

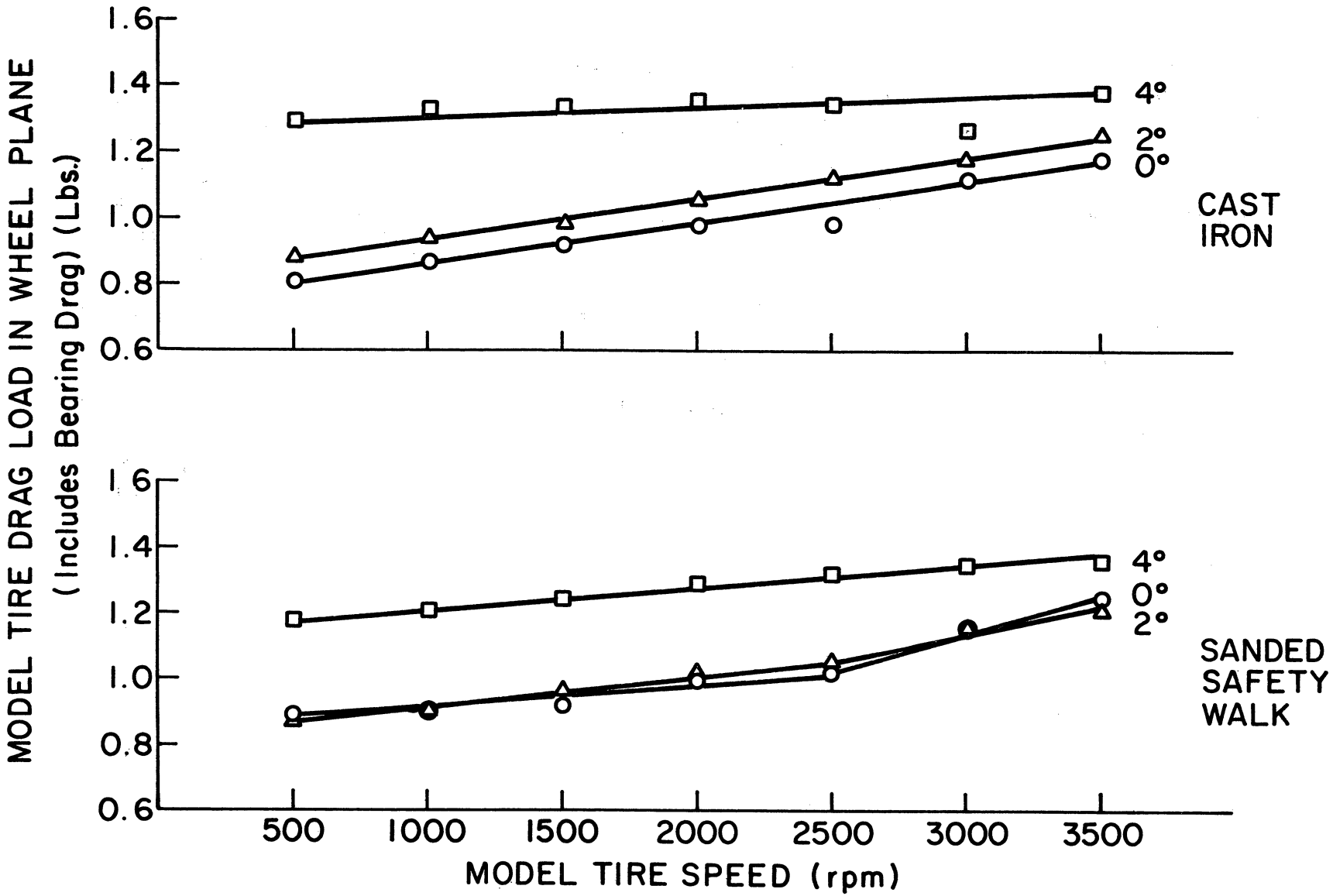

Figure 30. Drag load in wheel plane vs. speed.

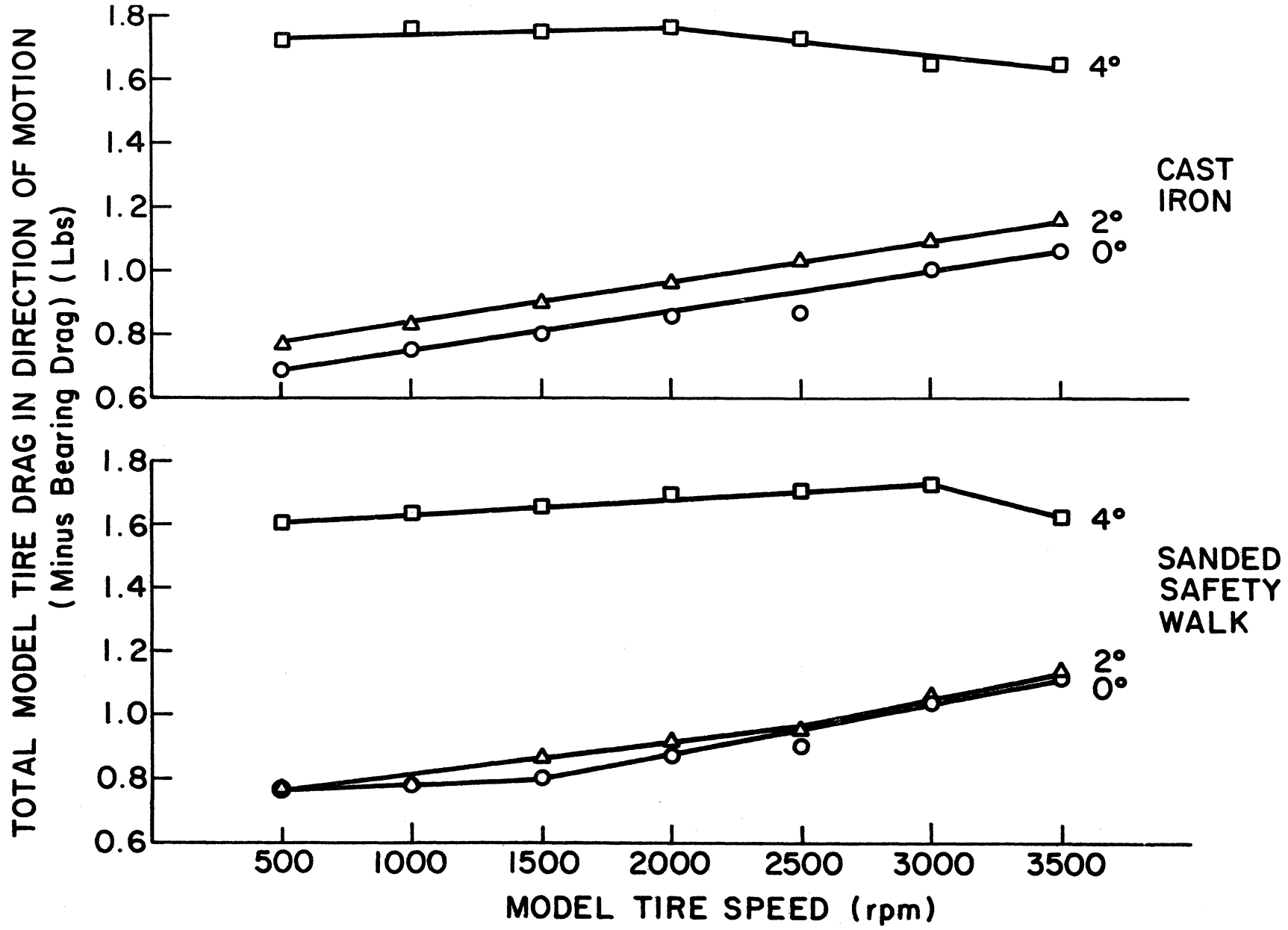

Figure 31. Drag load in direction of motion vs. speed.

VII. THERMAL ANALYSIS

This analysis is conducted in order to determine the temperature induced in the thin film of nickel of a sensor by the passage of a heat flux of length L at speed V at the outer surface of the sensor. The sensor is made of a thin film of nickel between two polyimide films, and this sensor is bonded to the road of different materials (see Figure 32 for dimensions).

The idealization of the problem is shown in Figure 33. q(t) represents the heat flux generated at the interface of tire with sensor, and we are looking for the temperature inside the layer of nickel due to the heat flux q(t). The function q(t) depends on the contact between tire and sensor, and if we assume a uniform heat flux q, we have

$$t = \frac{L}{V}$$

L: length of contact patch
V: speed of the vehicle
t: time of contact tire-sensor

The following assumptions are made in the analytical treatment of the problem:

(1) The problem is unidimensional.

(2) The thin flim of nickel is so thin and such a better conductor than polyimide that it can be eliminated.

(3) The layer of epoxy is supposed to be thin enough to be integrated to the road material.

The final model is shown in Figure 34.

We are looking for an expression of $\theta_1(x,t)$.

Equations and Solutions

Let us call $e_1 + e_3 = L$

the equations of conduction are

$$\begin{cases} \dfrac{\partial \theta_1}{\partial t} = \alpha_1 \dfrac{\partial^2 \theta_1}{\partial x^2} & -L \leq x \leq 0 \\ \dfrac{\partial \theta_2}{\partial t} = \alpha_2 \dfrac{\partial^2 \theta_2}{\partial x^2} & x \geq 0 \end{cases} \tag{2}$$

the boundary conditions are

$$\begin{cases} -k_1 \left(\dfrac{\partial \theta_1}{\partial x} \right)_{x=-L} = q & \text{(step function)} \\ -k_1 \left(\dfrac{\partial \theta_1}{\partial x} \right)_{x=0} = -k_2 \dfrac{\partial \theta_2}{\partial x} & x=0 \\ \theta_1(0,t) = \theta_2(0,t) & \\ \theta_1(x,0) = \theta_2(x,0) = 0 & \\ \theta_2(+\infty,t) = 0 & \end{cases} \tag{3}$$

Solving by Laplace transforms gives us

$$\begin{aligned} X_1(x,s) &= A\, e^{\sqrt{\frac{s}{\alpha_1}}\, x} + B\, e^{-\sqrt{\frac{s}{\alpha_1}}\, x} \\ X_2(x,s) &= C\, e^{\sqrt{\frac{s}{\alpha_2}}\, x} + D\, e^{-\sqrt{\frac{s}{\alpha_2}}\, x} \end{aligned} \tag{4}$$

A, B, C, D are determined with the boundary conditions and finally

$$\theta_1(x,t) = q\frac{\sqrt{\alpha_1}}{k_1}\left\{2\sqrt{\frac{t}{\pi}}\exp\left(\frac{-x^2}{4\alpha_1 t}\right)\sum_{n=0}^{+\infty}\frac{1}{k^n}\exp\left[\frac{-(2n+1)^2L^2}{4\alpha_1 t}\right]\right.$$

$$\left[\frac{1}{k}\exp\frac{(2n+1)L_{sc}}{4\alpha_1 t} + \exp\frac{-(2n+1)L_x}{4\alpha_1 t}\right] + \sum_{n=0}^{+\infty}\frac{1}{k^n}\cdot$$

$$\left.\left[\frac{x-(2n+1)L}{k\sqrt{\alpha_1}}\operatorname{erfc}\frac{(2n+1)L-x}{2\sqrt{\alpha_1 t}} - \frac{x+(2n+1)L}{\sqrt{\alpha_1}}\operatorname{erfc}\frac{(2n+1)L+x}{2\sqrt{\alpha_1 t}}\right]\right\} \quad (5)$$

Computer Program

The computer program calculates $\theta_1(x,t)$ for x = -L (outer surface) and x = -a (any position in the polyimide). The inputs are

(1) all thermal characteristics of the polyimide and the road material;

(2) the value L (called TH in the program) thickness of the polyimide;

(3) the value a (called POS in the program) position of the nickel film in the polyimide; and

(4) the shape of the heat flux q(t) in the form of a series of heat pulses (up to ten).

The program computes $\theta_1(-TH,t)$ and $\theta_1(-POS,t)$ using Duhormel's superprosition theorem.

The program itself and typical results are shown for a step function for q and different road materials: copper, aluminum, concrete, asphalt, micarta, in Figure 35.

```
0001              REAL*8 D,E,QK,F,G,O,P,Q,H,R,T,DEXP,DERFC,DSQRT,DABS,ST,TL
0002              DIMENSION X(2),T(90),F(200),Q(500),RES(90,2,21),ST(90),FRES(90,2),
                 1TP(20),U(20),V(21),TL(90,21)
0003              DATA V,U/21*0.,20*0./
0004            1 READ (5,100,END=999) CON1,ALP1,CON2,ALP2,TH,POS,TSVP,NP
0005          100 FORMAT(2E11.4/2E11.4/2E11.4/E11.4,I2)
0006              READ(5,201) M
0007          201 FORMAT(I2)
0008              DO 35 I=1,M
0009              READ(5,202) TP(I),V(I)
0010          202 FORMAT(2E11.4)
0011           35 CONTINUE
0012              W=0.
0013              DO 36 I=1,M
0014              W=W+TP(I)*(V(I)-V(I+1))
0015           36 CONTINUE
0016              IF(W.NE.TP(M)) GO TO 37
0017              TI=TSVP/NP
0018              X(1)=-POS
0019              X(2)=-TH
0020              A=SQRT(ALP1)/CON1
0021              B=2./SQRT(3.141596)
0022              C=CON2*SQRT(ALP1)/(CON1*SQRT(ALP2))
0023              QK=(1.+C)/(1.-C)
0024              DO 3 J=1,NP
0025              ST(J)=J*TI
0026              TL(J,21)=ST(J)/0.36E7
0027              DO 3 K=1,M
0028              IF(ST(J).LE.TP(K)) GO TO 4
0029              TL(J,K)=TL(J,21)-TP(K)/0.36E7
0030              GO TO 3
0031            4 TL(J,K)=0.
0032            3 CONTINUE
0033              DO 10 J=1,NP
0034              K=21
0035           63 T(J)=TL(J,K)
0036           62 DO 11 I=1,2
0037              IF(T(J).EQ.0.) GO TO 12
0038              G=0.
0039              H=0.
0040              R=(X(I)**2)/(4.*ALP1*T(J))
0041              DO 15 L=1,200
0042              N=L-1
0043              D=(2.*N+1.)*TH*X(I)/(2.*ALP1*T(J))
0044              E=((2.*N+1.)**2*TH**2)/(4.*ALP1*T(J))
0045              F(L)=(DEXP(D-E)/QK+DEXP(-D-E))/QK**N
0046              G=G+F(L)
0047              IF(L.EQ.1) GO TO 15
0048              IF(DABS(F(L)).LT.DABS(G)/1000.)  GO TO 17
0049           15 CONTINUE
0050              WRITE(6,101) ST(J),I
0051          101 FORMAT('1FIRST SERIES NON CONVERGENT AT TIME:',F7.3,'ON I=',I1)
0052              GO TO 79
0053           17 DO 20 L=1,500
0054              N=L-1
```

```
0055              U=(X(I)-(2.*N+1.)*TH)/SQRT(ALP1)
0056              P=(X(I)+(2.*N+1.)*TH)/SQRT(ALP1)
0057              Q(L)=(0*DERFC((-0)/(2.*DSQRT(T(J))))/QK-P*DERFC(P/(2.*DSQRT(T(J))
                 1)))/QK**N
0058              H=H+Q(L)
0059              IF(L.EQ.1) GO TO 20
0060              IF(DABS(Q(L)).LT.DABS(H)/1000.)  GO TO 22
0061           20 CONTINUE
0062              WRITE(6,102) ST(J),I
0063          102 FORMAT('1SECND SERIES NON CONVERGENT AT TIME:',F7.3,'ON I=',I1)
0064           79 RES(J,I,K)=0.
0065              GO TO 11
0066           22 RES(J,I,K)=A*(B*DSQRT(T(J))*DEXP(-R)*G+H)
0067              GO TO 11
0068           12 RES(J,I,K)=0.
0069           11 CONTINUE
0070              IF(K.EQ.21) K=0
0071              K=K+1
0072              IF(K.LE.M) GO TO 63
0073           10 CONTINUE
0074              IF(ST(1).GT.TP(1)) GO TO 37
0075              DO 41 K=1,M
0076              U(K)=V(K+1)-V(K)
0077           41 CONTINUE
0078              JK=1
0079              DO 43 J=1,NP
0080              IF(JK.EQ.M) GO TO 45
0081              IF(ST(J).GT.TP(JK)) JK=JK+1
0082           45 DO 43 I=1,2
0083              W=0.
0084              DO 44 K=1,JK
0085              W=W+RES(J,I,K)*U(K)
0086           44 CONTINUE
0087              FRES(J,I)=V(1)*RES(J,I,21)+W
0088           43 CONTINUE
0089              WRITE(6,106) CON1,ALP1,TH,CON2,ALP2,POS
0090          106 FORMAT('1','FIRST MATERIAL:CON1',8X,'ALP1',8X,'THICKNESS'/' ',15X,
                 13E11.4/' SECND MATERIAL:CON2',8X,'ALP2',8X/' ',15X,2E11.4/' POSITI
                 2ON OF NICKEL/INTERFACE=',E11.4)
0091              WRITE(6,204)
0092          204 FORMAT('0SHAPE OF HEAT FLUX'/'0',5X,'TIME',10X,'MAGNITJDE'/' ')
0093              DO 71 K=1,M
0094              WRITE(6,205) TP(K),V(K)
0095          205 FORMAT(' ',5X,F7.3,6X,E13.6)
0096           71 CONTINUE
0097              WRITE(6,103)
0098          103 FORMAT('0',10X,'TABLE OF TEMPERATURE OVER FLUX'/'0TIME IN THSEC',
                 14X,'TEMP/FLUX IN NICKEL',4X,'TEMP/FLUX AT SURF'/'0')
0099              DO 50 J=1,NP
0100              WRITE(6,104) ST(J),FRES(J,1),FRES(J,2)
0101          104 FORMAT(' ',2X,F7.3,9X,E13.6,10X,E13.6)
0102           50 CONTINUE
0103              WRITE(6,105)
0104          105 FORMAT('-','REMARK: UNIT OF TEMP/FLUX IS F-FT**2-HR/BTU')
0105            / GO TO 81
0106           37 WRITE(6,203)
0107          203 FORMAT('1ERROR ON FORM OF HEAT FLUX')
0108           81 GO TO 1
0109          999 CALL EXIT
0110              END
```

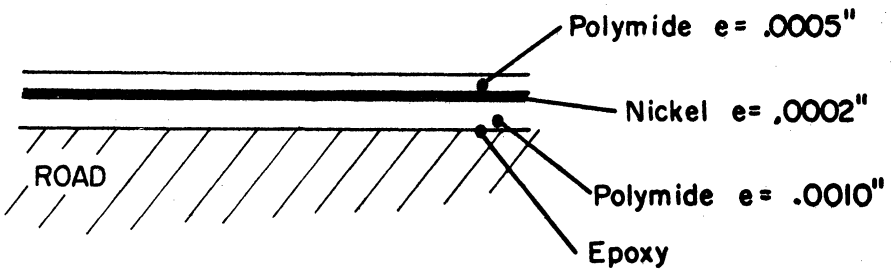

Figure 32. Detail of sensor installation.

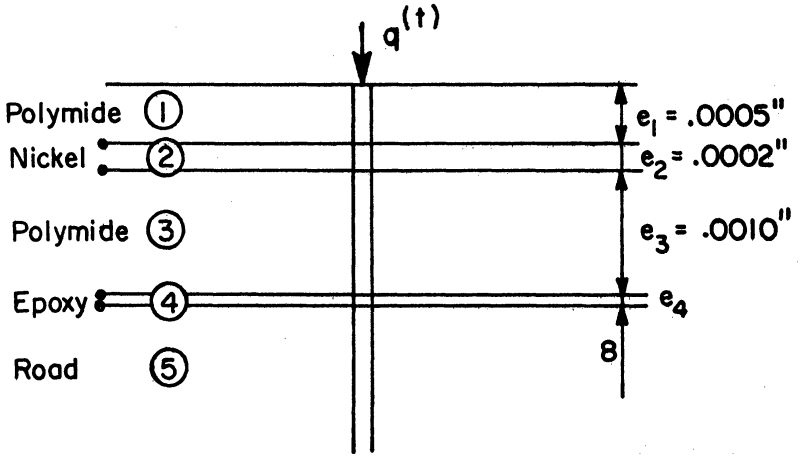

Figure 33. Schematic of sensor installation.

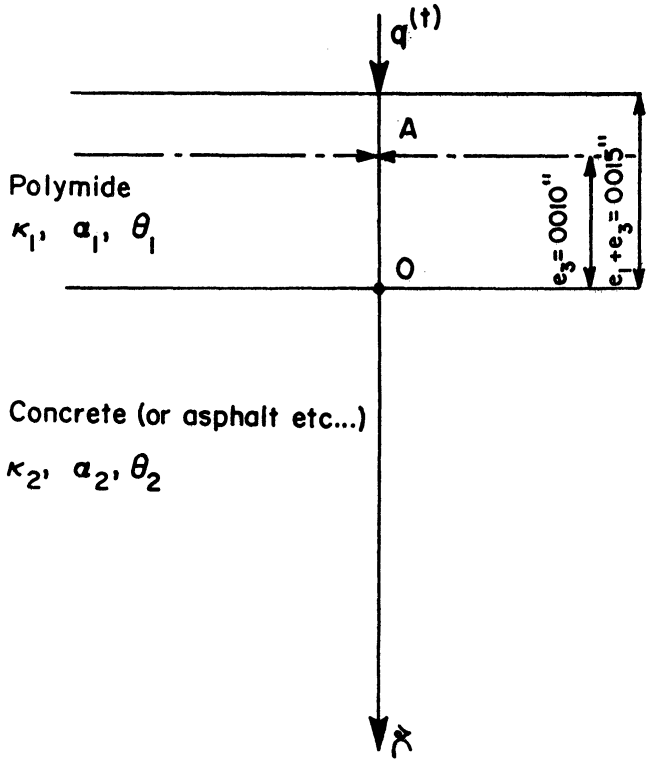

Figure 34. Analog of sensor installation for theoretical analysis.

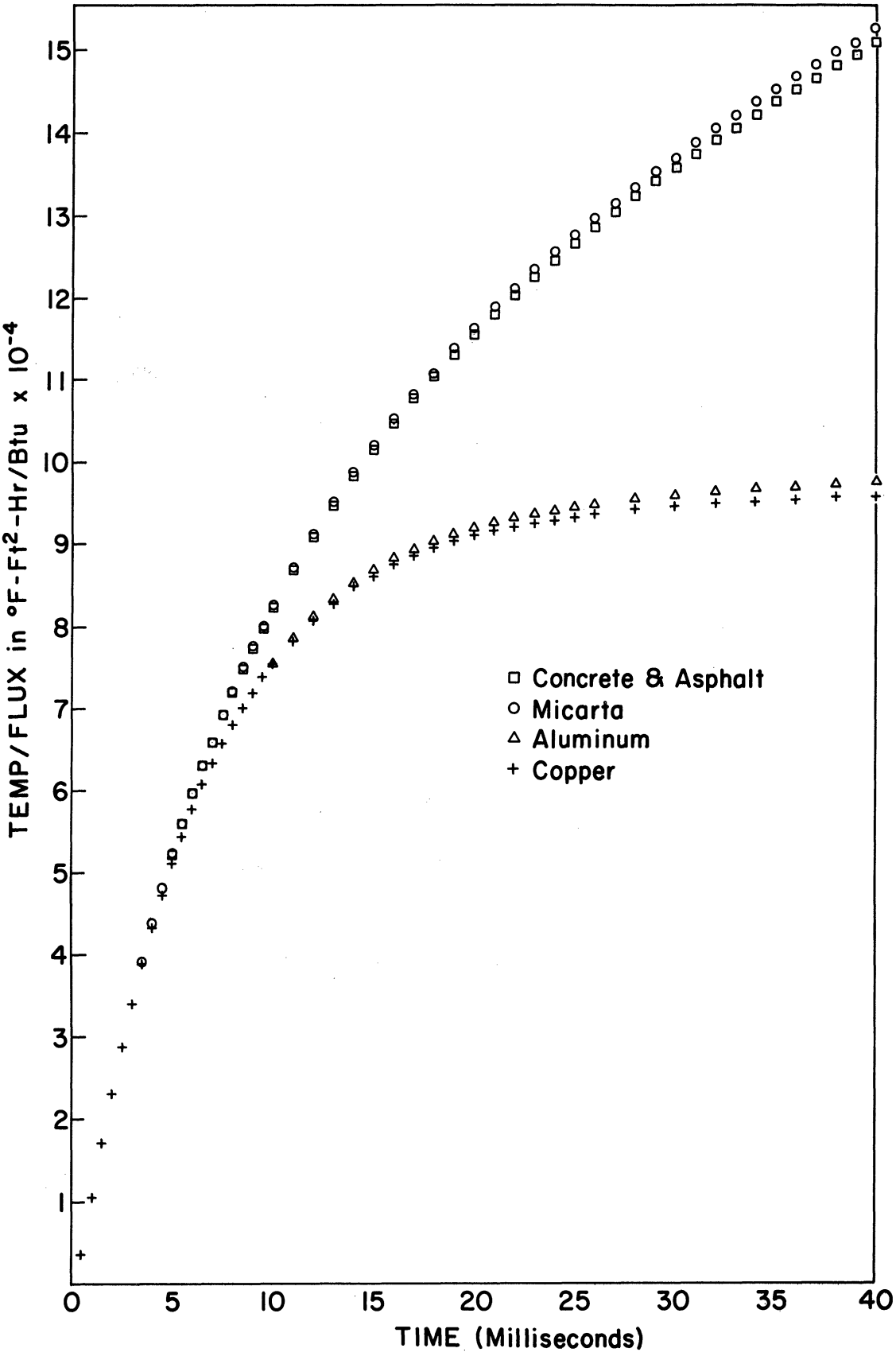

Figure 35. Temperature/flux in nickel as a function of time. First material: polyimide. Second material: as indicated.

VIII. REFERENCES

1. Yandell, W. O., "The Use of a Mechano-Lattice Analogy for Determining the Abrading Stresses in Sliding Rubber," Rubber Chemistry and Technology, 44, no. 3, June 1971, p. 758.

2. Viehman, W., "Surface Heating by Friction and Abrasion by Thermal Decomposition," Rubber Chemistry and Technology, 31, no. 4, 1958, p. 925.

3. Clark, S. K., R. N. Dodge, J. I. Lackey, and G. H. Nybakken, The Structural Modeling of Aircraft Tires, AIAA Paper No. 71-346, AIAA/ASME 12th Structures, Structural Dynamics, and Materials Conference, Anaheim, California, April 19-21, 1971.

4. Schallamach, A., "A Note on the Frictional Temperature Rise of Tyres," Journal of the IRI, 1, no. 1, January/February, 1967.

5. Seki, K., S. Sasaki, and H. Tsunoda, "Tyre Rolling Resistance," Automobile Engineer, pp. 88-91, March, 1969.

IX. APPENDIX

The second scheme for determining the total rate of heat generation involves partitioning the tire cross section into elements centered about their representative thermocouples. The elements are delineated by dashed lines in Figure 1. The sketch below illustrates this partitioning and the names assigned to the elements.

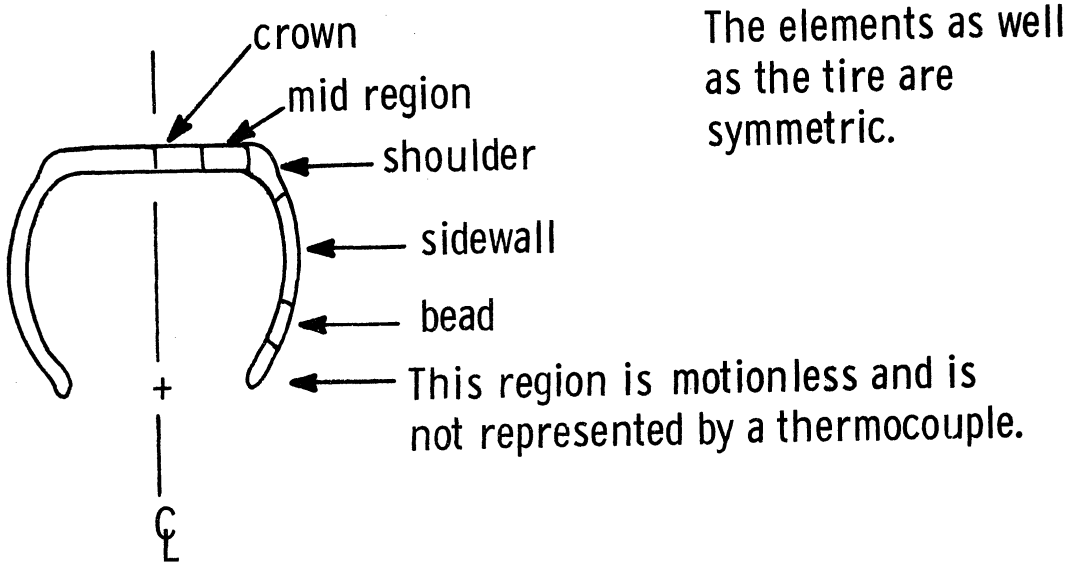

The areas of the elements and the approximate distances of the centroids from the scle center can be used to calculate the representative volumes. The percentage of the total volume represented by each element becomes a weighting factor in calculating a weighted sum of the rates of temperature increase. The tire is assumed to be homogeneous so that volume fractions are equivalent to mass fractions and the specific heat capacity is taken to be that of the rubber.

The figures given are for a G78-15. All thermocouples are 1/4 in. deep. The tire weighs 30 lb. The data is for a free rolling, 50 mph experiment.

Location	% Total Volume (Left + Right Sides)	Thermocouples Averaged	$\frac{\Delta T}{\Delta t}$ avg °F/sec
Actual Bead	5.1	none	0
Bead	8.7	1.9	.1063
Sidewall	22.3	2.8	.2125
Shoulder	26.9	3.7	.2032
Mid region	22.0	4.6	.1250
Crown	15.0	5	.1188

The weighted average is (5.1 x 0 + 8.7 x .1063 + ---) − 100 or .1566 °F/sec.

Then Q = .1566 x 30 x (.48 x 778) = 1750 ft lb/sec. The average of all the thermocouples 1-9 = .1570

$$Q = 1759 \text{ ft lb/sec.}$$

The agreement is quite good, compared to the nonweighted method of Section III of this report.